Mass flow and hydrofracturing during Late Devensian moraine emplacement, NE Scotland

Emrys Phillips* and Timothy I. Kearsey

British Geological Survey, The Lyell Centre, Research Avenue South, Edinburgh EH14 4AP, UK

* Corresponding author (erp@bgs.ac.uk)

Abstract

This paper presents the results of a detailed study of a sequence of Late Devensian (Weichselian) sands, gravels and diamictons exposed within a recessional moraine near Loch Killin near Fort Augustus, Monadhliath Mountains, NE Scotland. Macroscale sedimentological and structural field observations are combined with micromorphological and micro-structural analysis to investigate the ice-marginal processes which led to the construction of this landform. Microstructures present within the stratified diamictons mantling the glacitectonised core of the moraine reveal a complex history of microfabric development resulting from ductile shearing during the emplacement of these ice-marginal mass flow deposits. Shearing occurred throughout the entire mass flow with flowage occurring towards the WNW. The laminated sediments which infill a number of steeply inclined hydrofractures which cut the moraine are interpreted as having accommodated several phases of fluid flow, with a palaeoflow direction towards the WNW. A detailed model of ice-marginal landform development has been established involving glacitectonism as a result of ice-push during a readvance of the glacier (Stage 1), followed by mass flow of sediments released as a result of melting of the snout during a period of still stand (Stage 3), followed by hydrofracturing accompanying the escape of pressurised meltwater from beneath the ice, probably during the initial stages of glacier retreat.

Introduction

There are a range of processes, including bulldozing/pushing, squeezing, freeze on, melt-out and mass flowage of sediments, operating at the snouts of contemporary glaciers which result in the building of ice-marginal moraines on a variety of scales (e.g. Benediktsson *et al*., 2008; Benn and Evans, 2010; Bradwell *et al*., 2013). Ice marginal pushing leading to glacitectonism of penecontemporaneous or pre-existing sediments is generally regarded as the dominant process in the formation of annual recessional moraines. Such moraines are formed in response to the minor readvance of the ice margin during the winter, even though the glacier is undergoing overall retreat (e.g. Price, 1970; Sharp, 1984; Kruger, 1995; Evans and Twigg, 2002; Benn and Evans, 2010; Bradwell *et al*., 2013). However, melting of the ice at the snout during the summer months can lead to the deposition (dumping) of debris released from the ice to form ice marginal aprons and fans, which can themselves become deformed during a subsequent readvance (e.g. Hewitt 1967; Boulton and Eyles, 1979; Lukas, 2005, 2012). The sediment being released from the ice through melt-out will be subjected to remobilisation by mass flowage, gravity driven fall or even fluvial transport by meltwater streams. These so called "dump moraines" form were the ice remains stationary during the accumulation of the debris and their size will depend on the length of this still stand and volume of material being released from the ice (Benn and Evans, 2010). Consequently, the dominant moraine forming process can change both spatially and temporally along the ice margin leading to the construction of potentially complex ice-marginal landforms comprising both undeformed and highly tectonised glacigenic sediments. As a result the ice-marginal landforms preserved within the geological record may owe their origin to the complex interaction of a number of processes.

Although micromorphology has become a well-established technique and increasingly used by glaciologists and Quaternary geologists as a primary tool for the analysis of deformed glacigenic sequences and as an aid to understanding the processes occurring beneath glaciers (e.g. Menzies and Maltman, 1992; van der Meer, 1997; Menzies *et al*., 1997; Menzies and van der Meer, 1998; Khatwa and Tulaczyk, 2001; van der Meer et al., 2003; Roberts and Hart, 2005; Hiemstra *et al*., 2005; Baroni and Fasano, 2006; Larsen *et al*., 2006, 2007; Hart, 2007; Phillips *et al*., 2007, 2011, 2013a, 2018a, b; Denis *et al*., 2010; Narloch *et al*., 2012, 2013, 2020; Vaughan-Hirsch *et al*., 2013; Neudorf *et al*., 2013; Brumme, 2015; Spagnolo *et al*., 2016; Gehrmann *et al*., 2017; Evans, 2018), very few studies use this method to investigate the processes occurring in ice-marginal settings (e.g. Lachniet *et al*., 1999, 2001; Menzies and Zaniewski, 2003; Phillips, 2006; Reinardy and Lukas, 2009; Skolasińska *et al*., 2016). Consequently, our understanding of the microscale structures developed in response to ice-marginal processes (e.g. mass flow, freeze-thaw, desiccation and dewatering, fluvial reworking) remains limited. This is critical when these processes can strongly modify or even overprint any pre-existing features present within the sediments released from within, or beneath, the retreating ice. Furthermore, this lack of understanding becomes increasingly important when several published studies have tried to use micromorphology to determine the depositional setting of massive diamictons preserved within the geological record (van der Meer, 1987; Carr *et al*., 2000; Carr, 2001; Carr *et al*., 2006; Menzies *et al*., 2006; Kilfeather *et al*., 2010).

This paper contributes to our knowledge of the processes which led to the development of a Late Devensian (Weichselian) recessional moraine near Loch Killin in the Monadhliath Mountains to the east of Fort Augustus, NE Scotland (Fig. 1). Macroscale sedimentological and structural field observations are combined with micromorphological and micro-structural analysis to investigate the ice-marginal processes which led to the construction of this landform. Detailed mapping of the microstructures within the stratified diamictons and sands mantling the glacitectonised core to the moraine reveal a complex history of microfabric development formed as a result of ductile shearing during the emplacement of these mass flow deposits. Furthermore, thin sections taken from a system of sediment-filled hydrofractures which cut the moraine record the escape of pressurised meltwater from beneath the ice. Combining the results of both the macro- and microscale studies has allowed a detailed model of ice-marginal landform development to be established. This involved glacitectonism as a result of ice-push during glacier readvance, followed by mass flow of sediments released as a result of melting of the snout during a period of still stand, followed by hydrofracturing and water escape accompanied by extensional fault on the up-ice side of the moraine probably during the initial stages of renewed glacier retreat. The range of microstructures found within the mass flow deposits (diamictons) are comparable to those found within subglacially deformed traction tills which has important implications for anyone trying to use micromorphology, on its own, to establish the depositional setting of glacigenic diamictons.

Regional setting and location of study area

The exposed section examined during this study [NH 5190 1211] is located on eastern side of the River Fechlin which flows out of the northern end of Loch Killin, located to the west of Fort Augustus, NW Scotland (Fig. 1a and b). Loch Killin is an approximately NE-SW-trending, elongate lake filling a prominent steep-sided glaciated valley (Fig. 1c and d) on the north side of the Monadhliath Mountains. The bedrock geology in the study area is dominated by the polydeformed and metasedimentary rocks of the Grampian Group (Stephenson and Gould, 1995). In the northern and central parts of the area are underlain metamorphosed (amphibolite facies) sandstones belonging to the Loch Laggan Psammite Formation. However, in the southern part of the area, these micaceous metasandstones (psammites) are replaced by schistose metasiltstones (semipelites) of the Monadhliath Semipelite Formation. To the south of the study area the Grampian Group is intruded by the Devonian in age Allt Crom Granite.

In the Late Devensian, the Monadhliath Mountains occupied the central zone between corridors of relatively faster flowing ice (ice streams) moving north-eastwards along the Great Glen, to the north, and Strathspey, located to the south (Fig. 1c). During the early phases of the Late Devensian (28-22ka) the Monadhliath Mountains were believed to be entirely submerged by ice with the British and Irish

Ice Sheet (BIIS) extending offshore to merge with the Scandinavian ice occupying the North Sea basin (Bradwell *et al*., 2008; Merritt *et al*., 2013). However, ice on the Monadhliath massif itself is considered by Merritt *et al*. (1995, 2013) to have been either slow moving or cold-based, consequently it is unclear whether this area acted as an independent ice dispersal centre at any stage during the last glaciation.

During deglaciation, Boston and Lukas (2013) provided sedimentological evidence that suggested that Glen Killin was occupied by an ice-damned lake (also see Charlesworth, 1956; Boston, 2012). The modern day Loch Killin is constrained at its northern-end by a thick accumulation of unconsolidated glacigenic sediments. Exposed sections through this sequence occur on both the western and eastern banks of the River Fechlin [NH 524 113] (see Figs. 1d and 2). Immediately downstream of where the river leaves the loch, a section exposed on the western side of the river reveals a c. 8-9 m of glacifluvial outwash sands and gravels (Lithofacies (LFA) 1; Boston and Lukas, 2013) overlain by c. 1 m of laminated glacilacustrine clays (LFA2; Boston and Lukas, 2013), which are in turn being capped by a clast-rich diamicton which is interpreted as a subglacial traction till (LA3; Boston and Lukas, 2013). The mapped extent of these glacifluvial and glacilacustrine deposits are shown on Fig. 1d with the hummocky upper surface of the diamicton merging with the till covered slopes of the valley sides at approximately 400 m OD (Ordinance datum). A number of short (c. 50-100 m long), arcuate (convex down-valley), approximately NE-SW-trending crest lines which occur perpendicular to the river have been identified on the surface of these hummocky glacial deposits (Fig. 1d). Charlesworth (1956) argued that during deglaciation the lake formed as a result of damming the valley of the River Fechlin by ice flowing down from the north (see fig. 37 of Boston and Lukas, 2013). However, the size of the lake is disputed with Boston and Lucas (2013) arguing that it was large enough to drain into the valley of the River Eskin over a col at 642 m OD at the top of Glen Markie and into the head of the Findhorn Valley (Fig. 1d; also see Boston 2012). However, Merritt *et al*. (2013) concluded (based upon mapping by the BGS) that the ice dammed lake was less far extensive, reaching an elevation of no more than c. 500 m OD and that drainage occurred north-westwards through the valley of the River Fechlin.

Reconstructions of the younger, Younger Dryas ice sheet suggest the Monadhliath icefield terminated at the southern end of Loch Killin (Boston *et al*., 2015). Therefore it seems likely that the sections examined during the present study were unaffected by this later phase of ice advance.

Methods

Prior to sampling for micromorphology, the sedimentary sequence was logged and the macroscale characteristics, such as sedimentary lithofacies and architecture, and macroscopic deformation structures, were described and sketched in detail (Figs. 2 and 3), following the procedures prescribed in Evans and Benn (2004), Phillips and Lee (2011) and Evans (2018). The samples were collected using 10 cm square, aluminium Kubiena tins, which were cut into the face of each exposure in order to limit sample disturbance. The location, orientation, depth and way-up of the sample were marked on the outside of the tin during collection. Orientated samples are collected so that kinematic indicators (Passchier and Trouw, 1996; van der Wateren *et al*., 2000; Phillips *et al*., 2007), such as the sense of asymmetry of folds and fabrics, as well as the sense of displacement faults, could be established and used to provide information on the former stress regime. It is important that the orientation of the samples relative to the presumed direction of ice-push is established, as only thin sections cut parallel to this principal stress direction will exhibit the most complete record of deformation and its intensity. A total of 6 orientated samples were collected from the site: three samples (N13916 to N13918) of the finely laminated sands, silts and clays infilling a steeply inclined hydrofracture (Fig. 4a to e) which cuts the glacitectonised lake sediments which form the core of the moraine (Fig. 3a); and a further three samples (N13919 to N13921) were taken from a weakly stratified diamicton and underlying bedded sediments which mantle the western side of the recessional moraine (Figs. 3b and 4f).

Sample preparation (c. 10 months) involved the initial replacement of pore-water by acetone, which was then progressively replaced by a resin and allowed to cure. Large format orientated thin sections were taken from the centre of each of the prepared samples, thus avoiding artefacts associated with sample collection. Each thin section was cut orthogonal to the main structures evident from the field investigation. The thin sections were examined using a standard Zeiss petrological microscope. Detailed analysis of a sediment-filled hydrofracture was also carried out with the infill being divided into a number of lithological units (Figs. 5 to 10). Sedimentary logs through this laminated sand, silt and clay vein were constructed in order to highlight any systematic variation in the sediment type, sedimentary structures and layer thickness (Fig. 8). Further detailed microscale analysis of the clast microfabrics (coarse silt to small pebble sized clasts) developed within the stratified diamictons (Figs. 11 to 13) was carried out using the methodology of Phillips *et al*. (2011) (also see Vaughan-Hirsh *et al*., 2013; Neudorf *et al*., 2013; Gehrmann *et al*., 2017; Phillips *et al*., 2013, 2018a, b; Brumme, 2015). The clast orientation data are plotted on a series rose diagrams using the commercial software package StereoStat by Rockware™. During the microstructural mapping process the relationships between successive generations of clast microfabrics were determined, allowing the relative chronology of fabric development to be established (see Phillips *et al*., 2011 for details). Successive generations of fabrics (S1 or earliest to Sn last) were distinguished using the nomenclature normally used in structural geological studies (c.f. Phillips *et al*., 2007; Phillips and Lee, 2011).

Sedimentology and macroscale deformation structures within the moraine

The sedimentary and structural interpretation of the section exposed on northern-side of the River Fechlin is shown in Fig. 2. The section cuts through a thin (2 to 4 m thick) sequence of variably disrupted sands, gravels and diamictons, mapped as glacifluvial ice-contact deposits, which are overlain by hummocky glacial deposits (Fig. 1d). At the ESE-end of section the lower part of the sequence is composed of a folded and thrust sequence of sands and gravels (Figs. 2 and 3a). These sands and gravels are thought to correspond to the glaciofluvial outwash (LFA1) of Boston and Lukas (2013). The lowest exposed unit is a red-brown coloured, clast- to matrix-supported gravel composed of rounded to subrounded pebbles and cobbles of schistose metamudstone (c. 60%), metasandstone (psammite; c. 20%) and granite (c. 20%) within a matrix of coarse-grained micaceous sand. This is directly overlain by a complex sequence of disrupted lenses to irregular blocks of finely laminated (individual laminae 1 to 20 mm thick) sand and gravel (Figs. 2 and 3a). Although deformed, the sands locally preserve a moderately to well-developed cross-lamination with bedding dipping at low to moderate angles towards the SE (25° towards 134°). However, changes in the angle of dip and orientation of the bedding surfaces within the sands and gravels reveals the presence of a number of ESE-dipping thrusts (Fig 3a). The individual thrust planes are poorly defined and appear diffuse in nature. However, offset of bedding across these structures records a sense of displacement towards the WNW/NW; consistent with ice-push from the ESE/SE. In the centre of the exposure a sequence of thinly bedded sands and silts is deformed a number of ESE-dipping normal (extensional) faults (Fig. 3a) which locally appear to cross-cut and therefore postdate the earlier developed thrusts. At the eastern-end of the section the disrupted, lenticular bedding within the sands and gravels is deformed by a moderately inclined, WNW/NW-verging asymmetrical fold (Figs 2 and 3a). Minor folding within the core of this fold is complex to disharmonic suggesting that these sediments contained a high water content during deformation. The deformation structures within this glacitectonised unit, including a recumbent fold at the top of the deformed sequence, are truncated by the sharp, erosive base of a c. 60 cm thick unit of boulder gravel which fines upward into moderately to weakly bedded sand (Figs. 2 and 3a). The gravel locally contains imbricated pebbles and cobbles of metasandstone which record a palaeoflow direction towards the NW.

The glacitectonised sequence is cut by a number of steeply inclined (50° to 70°) ESE/SE-dipping sediment-filled veins (Figs. 4a and b). They range from 2 to 6 cm thick and can be traced laterally for up to 2-3 m. The veins are composed of thinly laminated sand, silt and clay with the lamination, which is locally lenticular in form, occurs parallel to the walls of the fracture (Figs. 4c and d). The margins of the veins are sharp and range from planar to irregular in form. These sediment-filled veins, interpreted as hydrofracture fills, are most common on the ESE-side of the exposed section where they clearly crosscut and therefore postdate the disruption as a result of glacitectonism. Comparable sediment-filled hydrofractures have also been recognised within the WNW-part of the section (see Fig. 2).

The central part of the section is composed of a massive, hard (overconsolidated) diamicton (possibly equivalent to LFA 2 of Boston and Lukas, 2013) which is cut by a c. 50 cm to 1m wide, steeply inclined to subvertical pipe-like feature composed of compact, closely packed (overconsolidated) gravel (Fig. 2). The contact between the diamicton and the adjacent glacitectonised sequence to the ESE is very steeply inclined to subvertical and appears to have been modified by the introduction of the gravel pipe. This boundary clearly crosscuts both bedding and the deformation structures within the glacitectonised part of the section. The contact between the diamicton and the bedded sequence exposed on the WNW-side of the section is observed by slope deposits and a cobble gravel; the latter representing recent fluvial deposits mantling the base of the section.

The sediments exposed at the WNW-end of the section are less disturbed and comprises a well-bedded sequence of sands, gravels and diamictons (Figs. 2 and 3b). The upper part of the sequence, however, is obscured by younger slope deposits (matrix-supported diamicton). The lowest part of the bedded sequence is composed of a matrix-supported gravel containing thin, lenticular interbeds of fine sand and clay which dip towards the NW. The gravel is poorly sorted and composed of sub-angular to rounded clasts of metasandstone, schistose metamudstone and minor granite (< 1%). The overlying lenticular unit (Fig. 2) is composed of laminated fine-grained sand with well-developed climbing ripple drift lamination towards the top. This is directly overlain by a coarse gravelly sand (Figs. 2 and 3b). Bedding within this part of the sequence dips gently towards the NW (16° towards 319°). This sequence of sands and gravels probably representing a least deformed equivalent to the glacitectonised glaciofluvial outwash observed in the ESE-part of the section (see Figs. 2 and 3b). The remainer of the sequence exposed in the WNW part of the section is composed of weakly bedded sands, gravelly sands and stratified diamictons. The diamicton layers are up to 1 m thick and comprise subangular to subrounded pebble sized clasts (same clast assemblage as the underlying gravels) within an apparently massive (on a macroscale) silty sand matrix. No obvious striated or faceted clasts were recognised within the diamicton. Bedding within this sequence is subhorizontal to very gently dipping towards the WNW (see Fig. 3b). The stratified nature of the diamictons coupled with presence of interbedded sands and gravels, and apparent absence of striated clasts has led to the conclusion that they represent mass flow deposits rather than a subglacial traction till.

Microscale structures within the sediment-filled hydrofractures

Three samples (N13916; N13917; N13919) were collected from a steeply inclined sediment-filled hydrofractures cutting through the glacitectonised glacilacustrine sequences within the core of the moraine (Fig. 4e). All three thin sections are composed of finely laminated clay, silt and sand filling a c. 3 to 8 cm wide, steeply ESE-dipping vein (75°ESE/019°; Fig. 4b) which cross-cuts an apparently massive, micaceous, matrix-poor sand (Figs. 5 to 7). In thin section the sand is fine-grained with a distinctive “mottled” appearance and lacking any obvious bedding or primary sedimentary structures. The moderately sorted, matrix-poor, open packed sand has a high intergranular porosity which is locally lined or filled by clay. These clay lined/filled pore spaces are most common immediately adjacent to the margins of the hydrofracture with the brown coloured clay being lithologically similar to the laminated silt and clay lining the walls of the fracture. The sand is composed of angular to subangular, low sphericity monocrystalline quartz and subordinate quartz fragments. Needle-like to tabular flakes of muscovite and biotite are a common minor detrital component, and exhibit a locally well-developed preferred shape alignment defining an irregular to anastomosing fabric which is apparently coplanar to the margins of the sediment filled vein (Figs. 5 to 7).

The sediment-filled hydrofractures are composed of finely laminated silt and clay along their margins (units 1 and 3 on Figs. 5 to 7) with the central part of the vein composed of a slightly coarser grained fill of sand and silt (unit 2 on Figs. 5 to 7). The margins of the vein are sharp, ranging from planar to slightly irregular in form. However, if the sediment-fill was removed the margins of the hydrofracture will not fit together suggesting that there has been some erosion of the side-walls. The clays immediately adjacent to the wall of the hydrofracture possess a locally well-developed plasmic fabric which occurs coplanar to the side-walls which is defined by optically aligned clay minerals. The clays are also deformed by number of small-scale extensional (normal) faults defined by a well-developed unistrial plasmic fabric. The sense of movement across these faults towards the ESE consistent with sediment being displaced/collapsing into the open facture.

Detailed graphic logs through the sedimentary fill observed in thin section are shown in Fig. 8. The laminated clay and silt along the structurally lower margin (unit 1) of the hydrofracture locally form discrete couplets which fine upwards (“normal” grading) (see Figs. 8, 9 and 10). However, adjacent to the upper margin (unit 3) this grading is reversed with both clay-silt-rich marginal sequences fining towards the centre of the hydrofracture (see Fig. 8a). The thicker lenses and laminae of silt within the marginal sequences and thicker sand layers within the centre of the vein are cross-laminated (Figs. 9 and 10) and record a consistent palaeoflow direction “upwards”, towards the WNW (Figs. 5 to 8; also see Fig. 4b). The cross-laminated silt lenses within the clay-rich marginal sequences may represent isolated ripples which migrated upwards along the open fracture. The foresets are locally deformed and possess a distinct S-shaped to curved geometry (see Figs. 9 and 10) with the asymmetry of these folded foresets recording an apparent WNW-directed sense of shear, consistent with the palaeoflow direction. The bases of the sand layers are sharp and vary from planar to irregular, with the latter clearly eroding into the underlying sediments (Figs. 8, 9 and 10). Small-scale load structures were also noted on the bases of some of the sand and silt layers. The composition of the sand laminae within the hydrofracture is comparable to that of the host sediments, with these host sands also filling small late stage veinlets which crosscut the larger hydrofracture (Figs. 5, 6 and 9a).

Microstructures within the stratified diamictons and sands

In thin section sample N13919 is composed of weakly to moderately, thinly bedded coarse-sand, silty and silty sand which can be divided into four main units (Fig. 11): (i) occurs at the bottom of the thin section and comprises poorly sorted coarse silt with graded silt to clay laminae indicating that the sequence is the right-way-up; (ii) the overlying unit of matrix-supported, poorly sorted and weakly laminated coarse-grained silty sand; (iii) a laterally discontinuous, lenticular layer of laminated coarse silt to fine sand; and (iv) a fining upwards unit of weakly laminated, poorly sorted sand and silty sand. Angular to subangular, low sphericity sand to granule sized clasts within the coarser-grained layers are mainly composed of monocrystalline quartz and metasedimentary rock fragments. Minor to accessory detrital components include garnet, muscovite and biotite. The detrital assemblage within these sandy sediments indicating that the sediment is locally derived from the Grampian Group. The stratified and locally graded nature of these sediments is consistent with them being deposited by meltwater.

Samples N13920 (Fig. 12) and N13921 (Fig. 13) were taken from the overlying diamicton; sample N13920 from near to the base and N13921 from higher up within this c. 1 m thick, apparently massive (macroscopically) deposit. In thin section the diamicton is a coarse-grained, texturally and compositionally immature, open-packed and matrix-supported deposit containing angular to subangular lithic clasts of locally derived metasedimentary rocks including garnet-biotite-schist, biotite-metasandstone, hornfelsed biotite-schist and quartzite, as well as biotite-granite (Figs. 12 and 13). The fine silty sand matrix to the diamicton is micaceous with biotite and muscovite being common minor detrital components. Sand to coarse silt grains within the matrix are mainly composed of monocrystalline quartz with subordinate amounts of plagioclase. A moderately to well-developed preferred shape alignment of the elongate sand grains and, in particular, detrital micas is locally developed within the matrix. However, no obvious plasmic fabrics have been recognised probably reflecting the relatively low modal proportions of clay minerals within the matrix to the diamicton. A number of the larger granule to pebble sized clasts are enclosed within a "halo" of finer grained, silty matrix.

Microstructural analysis of the thin sections has revealed that the tills possess four successive generations of clast microfabric defined by the preferred shape alignment of elongate coarse silt to sand-grade clasts: (i) the earliest fabric (S1) is a subhorizontal to gently WNW-dipping (in the plane of section represented by the thin sections) foliation (brown on Figs 12. and 13); (ii) this fabric is cross-cut by a moderately (S2a) to steeply (S2b) WNW-dipping foliation (dark green; Figs. 12 and 13); (iii) a third (S3) moderately inclined ESE-dipping foliation (pale green; Figs. 12 and 13) which appears to cross-cut both of the earlier foliations; and (iv) the latest fabric is a weakly developed subvertical foliation (S4) (orange-brown; Figs. 12 and 13). The S1 and S3 fabrics are the dominant foliations with the relative intensity of these microfabrics varying across the sample reflecting the heterogeneous nature of deformation. The spacing of the microfabrics is controlled by the overall grain size of the diamicton with the large, granule to pebble-sized clasts acting as rigid bodies and controlling the partitioning deformation within the matrix. Asymmetrical (S-shaped) fabric geometries defined by both S1 and S3 record a consistent sense of shear towards the NW (see Figs. 12 and 13). In contrast to these earlier shear related fabrics, the later S4 foliation which clearly cross-cuts all the earlier developed clast microfabrics is thought to have possibly formed during the dewatering of the sediment. The rose diagrams on Figs. 12 and 13 indicate that although the relative intensity of S1, S2 and 3 vary in different parts of the thin section, the dip of these microfabrics appears to remain relatively consistent throughout the c. 1 m thick deposit.

Interpretation

Sedimentation in response to fluid flow within the hydrofractures

The laminated nature of the sediment-fill and the presence of locally well-developed/preserved sedimentary structures (Figs. 8, 9 and 10) clearly indicate that the steeply inclined hydrofractures which cut the ice-marginal moraine at the northern-end of Loch Killin accommodated several phases of fluid flow. Comparable with other sediment-filled hydrofracture systems in glacial environments (e.g. van der Meer *et al*., 2009; Phillips *et al*., 2013b; Phillips and Merritt, 2008; Phillips and Hughes, 2014) the earliest sediments laid down along the margins of the vein being a thinly laminated sequence of clay and silt which fines towards the centre of the fracture (see Fig. 8). The presence of a well-developed plasmic fabric within the clay immediately adjacent to the fracture wall has previously been interpreted as recording the "plastering" of the clays onto the margins of the open/active hydrofracture (Phillips *et al*., 2013; Phillips and Hughes, 2014). These laminated clay-rich layers may be analogous to “mud cake” which form during drilling of hydrocarbon wells and boreholes (e.g. Feng *et al.*, 2015). Mud cake forms as fine particles present within the drill mud are filtered out and deposited on the inside of a borehole as the suspending fluid seeps into the surrounding porous rock. The two main conditions for mud cake development are: (i) a high solids content within the fluid being injected; and (ii) initially high rates of fluid penetration through the wellbore into the surrounding rock or sediment (Feng *et al.*, 2015). Once formed, however, mud cake forms a low permeability barrier preventing further penetration and fluid loss. A similar model can be applied to the development of the clay-rich layers lining the walls of hydrofracture systems in glacial environments. Leakage of fluid during the early stages of hydrofracture development is suggested by the presence of clay within the intergranular pore spaces of the sand immediately adjacent to the fracture. The development of these clay linings and/or pore filling cements would have reduced the permeability of these matrix-poor sediments. This reduction in porosity/permeability, coupled with the filtering and deposition of an extremely low permeability clay layer along the walls of the hydrofracture, would have effectively confined further fluid flow and/or subsequent flow events to within this evolving system.

The sand forming the walls of the hydrofracture possesses a well-developed, irregular to anastomosing foliation defined by shape-aligned detrital biotite and muscovite (Figs. 11, 12 and 13). Importantly this steeply inclined detrital mica foliation occurs parallel to the margins of the hydrofracture. Furthermore, at both a macro- (Fig. 4c) and microscale (Figs. 5 to 7) the sand adjacent to the hydrofracture possess a distinctive mottled appearance, typically associated with the liquefaction and homogenisation of unlithified glacial sediments (references). The sand also lacks of any obvious bedding or any other primary sedimentary structures which were potentially overprinted as homogenisation as a result of localised liquefaction. There is no clear relationship between the mica foliation and any macro- or microscale soft-deformation structures (folds, faults and ductile shears) which formed as a result of glacitectonism. As a result the mica foliation is interpreted as having formed due of the realignment of the needle-like to tabular detrital grains in response to intergranular fluid flow (see Figs. 5 to 7) which led to the overprinting of the primary (depositional) texture/structure of the sand. Analysis of samples N13916, N13917 and N13918 suggests that the sediment-filled hydrofracture cross-cuts and, therefore, postdates the formation of this mica foliation (Figs. 5, 6 and 7, respectively). Consequently, intergranular fluid flow through the sand may have occurred in association with an earlier phase of water-escape from beneath the ice. The pressure of the submarginal to subglacial hydrodynamic system is then thought to have changed, possibly increasing dramatically, thereby exceeding the cohesive strength of the sand leading to hydrofracturing. Subsequent, fluid flow and water-escape would have then been confined to within the clay-lined hydrofractures.

Detailed logging of the sediment-fill has revealed the presence of both fining and coarsening upward sequences (Fig. 14) thought to reflect changes in the velocity of fluid flow through the active hydrofracture system (cf. Phillips *et al*., 2013; Phillips and Hughes, 2014). Cross-cutting relationships between the sand and silt layers, coupled with the presence of erosive bases to these layers are consistent with the hydrofracture having accommodated several phases or pulses of fluid flow and accompanying sedimentation. As noted above, the cross-lamination within the silts and sands record a consistent palaeoflow direction upwards through the hydrofracture towards the WNW (Figs. 4b, 5, 6, 7 and 8). The cross-laminated silt lenses within the clay-rich marginal sequences may represent isolated ripples which migrated upwards along the open fracture; possibly reflecting changes in the volume of sediment being transported through the system (cf. starved ripples?). The development of sedimentary structures (graded bedding, cross-lamination…etc.) within the sedimentary fill to the hydrofracture indicates that this system was “open” during the period of fluid flow with the pressurised meltwater being able to escape its far end (Jeff Peakall, pers. comm. 2018), for example onto the surface of the landform. Consequently, the hydrofracture can be viewed as acting as a “confined” fluviatile-like system enabling a mix of pressurised meltwater and sediment to escape from beneath the ice feeding a so called “burst out” structure of Benediktsson *et al*. (2008). The sediment-filled veins have not been tilted/deformed subsequent to their formation (see Figs. 4 a, c and d), consequently the ripples were actively climbing up a steeply inclined (c. 75°), open hydrofracture (Fig. 14). The foresets typically dip at an angle of < 30° to the margin of the vein, i.e. at a lower angle than the typical angle of repose (c. 30-35°) of foresets associated with climbing ripples (Figs. 9 and 10). This lower angle of repose is thought to relate to the fact that the ripples are confined and climbing up the steeply inclined hydrofracture. Locally the foresets are deformed and possess a distinct S-shaped to curved geometry with the asymmetry of these folded foresets recording an apparent WNW-directed sense of shear, i.e. consistent with the palaeoflow direction recorded by the cross-lamination.

Figure 14 is a conceptual model illustrating the progressive infilling of an active hydrofracture system due to the stacking of individual layers or lenses of sand and silt. The lenticular nature of bedding observed in thin section (see Figs. 9 and 10) suggests that deposition was localised with the cross-laminated sands migrating upwards along the active hydrofracture (Stage 1; Fig. 14), possibly taking a form similar to that of starved ripples (Stow, 2007). Lenses of cross-bedded silt and/or sand may represent individual packages of sediment or ripples which migrated upwards through the hydrofracture with deposition occurring as a result of falling water pressure. The sedimentary sequence within the hydrofracture is built up as a series of sediment packages with successive ripples climbing up the lee-side of earlier formed deposits (Stages 2 to 4; Fig. 14). Each phase of deposition is typically marked by a sharp, erosive surface at the base. The foresets are locally deformed by

WNW/NW-verging folds consistent with a sense of shear “upwards” along the hydrofracture. Consequently, this localised soft-sediment deformation is thought to occur as a result of shear induced by flow of overpressurised fluid (sediment and water) across wet, deformable sediment leading to the localised folding of foresets within earlier formed cross-laminated units (Stage 3; Fig. 14). It is possible that the laminated sediment fill may represent several phases of deposition during a single prolonged flow event in which flow velocity/water pressure fluctuated leading to the observed changes in grain size…..etc. Alternatively each unit represents a single flow event within the hydrofracture with the entire sequence being built up over time as a result of several phases of fluid flow.

Synsedimentary deformation associated with mass flow emplacement

The macro- and microscale observations of the stratified diamictons and sand sequence which mantles the north-western side of the moraine are consistent with these sediments being laid down as a result of ice marginal sedimentation. The thinly bedded to laminated nature of the sand, silt and clay observed in thin section (N13919) coupled with the presence of weakly developed fining upward sequences (Fig. 15) may be consistent with these sediments being water lain. However, the matrix-supported, massive (no obvious crossbedding…etc.) nature of the poorly sorted, coarse to fine sands (Fig. 11) may indicate that they were more likely to have been deposited as a water-rich slurry on the surface of the moraine rather than from a body of water (e.g. river or lake). The composition and coarse-grained nature of the overlying diamictons clearly indicates that these sediments were locally derived and were being released as ice melted at the snout from the melting ice at the glacier snout. The thin sections obtained from the diamicton provide a valuable insight into the processes occurring during the emplacement of these deposits.

The clast microfabrics identified within the diamicton (N13920; N13921) are considered to have developed as a result of the partitioning of deformation into the matrix of the mass flow deposit (see Fig. 15). Although cross-cutting relationships have been identified between the various generations of fabrics (Figs. 12, 13 and 15), it is likely that S1 to S3 developed in response to the same overall stress regime. The relationships between these microfabrics clearly indicate that ductile shearing occurred throughout the entire mass flow and led to the development of P and R-type Reidel shears (Fig. 15). Consequently this microscale evidence may provide important evidence regarding the nature of the mass flow and its mode of emplacement (see Lawson, 1982; Lachniet *et al*., 1999; Phillips, 2006; Reinardy and Lukas, 2009). Lawson (1982) and Lachniet *et al*. (1999) recognised four different types of mass flow formed within contemporary ice-proximal environments: Type 1 flows a have a water content of 8-14% by weight, are lobate in shape and composed of a cohesive mass flowing over a few centimetres thick basal shear zone; Type 2 flows, with a water content of 14–19%, are commonly channelised, and move as a cohesive mass over basal and lateral shear zones; Type 3 flows have a water content of 18–25%, are once again channelised, but flow by differential shear throughout; whereas Type 4 flows contain a water content of >25% water, may be liquefied, and transport occurs by laminar flow with shear throughout. Consequently, the occurrence of shear related microfabrics throughout the River Fechlin diamicton may be used to tentatively suggest that these deposits can be characterised as a wet sediment Type 4 flow of Lachniet *et al*. (1999) (also see Lawson, 1982). The sense of shear recorded by the microfabrics is consistent with a direction of flow towards the WNW, probably as a result of mass flowage down the inclined, down-ice dipping surface of the moraine. This interpretation is consistent with the field observation that bedding within this part of the exposed sequence dips gently towards the WNW/NW (see Figs. 2 and 3b). If correct then it suggests that the ice mass providing the source of the mass flows was located to the ESE/SE.

Discussion

Interplay between glacitectonics, hydrofracturing and ice marginal sedimentation during construction of a recessional moraine

The dominant moraine forming process can change both spatially and temporally potentially leading to the construction of complex ice-marginal landforms which owe their origin to the complex interaction of a number of processes. The results presented here of a macroscale (field) sedimentological and structural study, combined with a detailed micromorphological analysis, have provided valuable insights into the ice-marginal processes which interacted during the construction of the moraine exposed near Loch Killin.

The exposed section through the moraine reveals that it is composed of three main components and that the complexity of deformation increases towards the ESE/SE (Fig. 2). The most intensely deformed sediments occur on the ESE-side of the section (Figs. 2 and 3a). The geometry of a mesoscale asymmetrical fold deforming bedding within the sands and gravels, coupled with the observed SE-directed sense of displacement across the thrusts records a direction of ice-push towards the WNW/NW (Stage 1, Fig. 16). This indicates that ice advanced was from the SE with the deformed sequence probably occurring close to the ice-contact slope. The complex, disharmonic nature of the minor folds suggested that these sediments may have been water saturated at the time of deformation. The core of the moraine is composed of a massive, compact (hard) diamicton which is cut by a vertical pipe of over consolidated gravel (Fig. 2). The diamicton and deformed outwash sands and gravels were probably stacked together within the moraine during the early stages of the construction of this landform (Stage 1, Fig. 16). It is possible that the gravel was injected into the diamicton and may have formed the feeder to a "burst out" structure associated with the escape of pressurised meltwater (c.f. Benediktsson *et al*., 2008). However, due to the nature of the exposure it has not been possible to establish the relative timing of this injection event.

The sediments of the WNW-side of the moraine are relatively undeformed with bedding on this side of the landform gently dipping towards the WNW/NW (Fig. 2 and 3b). These sediments are interpreted as ice-marginal glacifluvial sand and gravels that may either: predate moraine construction and represent the undeformed equivalents of the glacitectonised sequence located immediately to the ESE; or alternatively, may be penecontemporaneous with moraine construction and deposited by meltwater streams emanating from the snout (see Stage 2, Fig. 16). The coarse-grained nature of these sediments coupled with the presence of climbing ripples within the sands is consistent with an ice-marginal position and relatively high sedimentation rates. If this interpretation is correct then the dip of the bedding towards the WNW may preserve the palaeoslope located on the down-ice side of the moraine (Stage 2, Fig. 16).

The stratified diamictons and gravelly sands which overlie the outwash are interpreted as ice-contact mass flow deposits (Stage 2, Fig. 16). Thin sections obtained from the diamictons and interbedded sands provide a valuable insight into the processes occurring during the emplacement of these deposits. The thinly bedded to laminated nature of the sands (N13919) coupled with the presence of weakly developed fining upward sequences (Fig. 15) are consistent with these sediments having been water lain, possibly as a water-rich slurry flowing down the front of the moraine. The composition and coarse-grained nature of the overlying diamictons clearly indicates that these sediments were deposited in an ice-proximal setting, sourced by locally derived detritus being released due to melting at the snout during a period of still-stand (Stage 2, Fig. 16). Clast microfabrics within the diamicton (N13920; N13921) record the partitioning of soft-deformation within the matrix during emplacement with ductile shearing occurring throughout the entire mass flow (Fig. 15). This microscale evidence, when compared with the published literature (Lawson, 1982; Lachniet *et al*., 1999; Phillips, 2006; Reinardy and Lukas, 2009), may be used to suggest that these deposits represent Type 4 wet sediment (water-rich) flows of Lachniet *et al*. (1999) (also see Lawson, 1982). The kinematics recorded by the shear related microfabrics are consistent with a direction of flow towards the WNW (see Fig. 15), providing further evidence for the presence of a palaeoslope on the down-ice side of the moraine, with the glacier snout located immediately to the ESE/SE (Fig. 16).

Both the glacitectonised sequence on the up-ice of the moraine and the undeformed sediments on its WNW-side are cut by a number of ESE/SE-dipping sediment-filled hydrofractures (Figs. 2 and 16). These features clearly crosscut the glacitectonic folds and thrusts indicating that they formed at a later stage in the development of the moraine and record the release of pressurised meltwater from beneath the ice (Stage 3, Fig. 16). The laminated nature of the sediment-fill clearly indicates that the hydrofractures accommodated several phases of fluid flow with the locally well-developed/preserved cross-lamination recording a palaeoflow direction towards the WNW consistent with pressurised meltwater escaping upwards through the active/open fracture system. Studies of the subglacial hydrogeology of modern glaciers and ice sheets have shown that meltwater discharge varies on a range of scales from daily, to yearly, to longer decadal cycles (Hubbard *et al*., 1995; Boulton, 2006; Benn and Evans, 2010 and references therein). Consequently, the complexity of the sediment-fill may indicate that the hydrofractures were active over a prolonged period, possibly days or even months.

The presence of a well-developed, irregular to anastomosing foliation defined by shape-aligned detrital biotite and muscovite within the sands hosting the hydrofracture indicates that fluid flow was initially intergranular led to the localised overprinting of the primary (depositional) texture/structure of these sediments. The pressure of the hydrodynamic system then appears to have changed, possibly increasing dramatically and exceeding the cohesive strength of the sand leading to hydrofracturing. The thin sections reveal that fluid leaked into the host sand during the early stages of fracture development blocking the pore spaces reducing its permeability. The associated filtering and deposition of an extremely low permeability clay layer (cf. mud cake in hydrocarbon wells; Feng *et al*., 2015) lining the fracture walls would have confined further fluid flow and/or subsequent flow events to within the hydrofracture system. On the up-ice side of the moraine the sediment-filled hydrofractures are spatially related to a set of normal faults (see Fig. 3a). Consequently, it can be argued that hydrofracturing may have accompanied extensional faulting and minor collapse of the up-ice side of the moraine possibly during the initial stages of retreat of the glacier (Stage 3; Fig. 16). Extensional deformation would have also facilitated deposition of the sediment-fills by providing the required accommodation space with the repeated movement (slip) on the faults promoting reactivation of the hydrofractures.

In summary, combining the results of both the macro- and microscale studies has enabled a detailed model of ice-marginal landform development to be established. Construction of the moraine located to the north of Loch Killin can be divided into three stages: *Stage 1* equates to the initial advance of the glacier with the associated WNW/NW-directed ice-push leading to glacitectonism of a pre-existing sequence of diamictons and glacifluvial outwash; this was followed by *Stage 2* which led to the deposition of a sequence of ice-marginal glacifluvial and mass flows deposits, possibly during a period of still-stand which was accompanied by melting and down wasting of the snout; and finally *Stage 3* which is characterised by the development of a network of sediment-filled hydrofractures which allowed overpressurised meltwater to escape from beneath the ice onto the surface of the landform, possibly during the initial stages of retreat (Fig. 16).

Implications for the deglaciation of the Loch Killin area

The glacigenic deposits at the northern-end of Loch Killin record part of the history of deglaciation within the glen. Boston and Lukas (2013), following Charlesworth (1956), argued that during deglaciation a large proglacial lake formed as a result of damming the valley of the River Fechlin by ice flowing down from the north (also see Boston 2012). As highlighted above this interpretation was contested by Merritt *et al*. (2013) who considered that this ice-dammed lake was less far extensive, and that it drained north-westwards through the valley of the River Fechlin. Evidence presented here clearly points to ice having occupied the glen to the south of the exposed sections on the banks of the River Fechlin. The exposed glacigenic sediments and geomorphology appear to record the southward retreat of this "Loch Killin glacier", with the proposed history of deglaciation of the Loch Killin area being shown in Fig. 17.

During the early stages of retreat, melting of the glacier led to the deposition of a locally thick sequence glacifluvial deposits exposed at the northern-end of Loch Killin. Deposition of these ice-marginal to proglacial sands and gravels was punctuated by several phases of readvance. A series of linear to arcuate (convex down valley) crest lines, orientated across the glen (Figs. 1d and 17), are interpreted as marking these minor readvance limits. The section examined during this present study provides detailed evidence of the ice marginal process occurring during the construction of these recessional landforms. Initial construction of the moraine occurred as result of ice-push towards the WNW/NW (Stage 1, Fig. 16) consistent with ice occupying the valley to the ESE/SE (Fig. 17a). The mapped distribution of the hummocky glacial deposits in this part of the glen (Fig. 1d) suggests that the glacier may have expanded to fill the valley, possibly advancing north-eastwards up the relatively gentle slope on this side of the valley (Fig. 17a). However, the absence of any obvious ice-marginal landforms in this area means that the ice limit on this side of the valley is poorly constrained.

Initial advance was followed a period of still stand and ice-marginal sedimentation with the melting ice releasing sediment which fed a sequence of mass flows and interbedded sands and gravels (Fig. Stage 2, 16). The exposed section coincides with a crest line further up the valley side, as well as a much longer linear crest line located on top of a bedrock cored spur on the west side of the valley (Fig. 17a, also see Fig. 17d). This spur forms a constriction in the valley and occurs at the point at which the glen abruptly changes orientation from NW-SE to NE-SW (Fig. 1d). This narrowing and change in orientation of the valley may have limited the readvance of the Loch Killin glacier, which may have stabilised on the underlying spur (Fig. 17a), promoting a period of still-stand and observed ice-marginal sedimentation. As the ice began to retreat from this readvance limit, normal faulting on the ice-contact side of the recessional moraine would have facilitated the escape of overpressurised meltwater from beneath the ice (Stage 3, Fig. 16).

As the ice retreated it left behind a mixed sequence of glacigenic deposits composed of outwash sands and gravels, subglacial traction tills and mass flow deposits; collectively mapped as hummocky glacial deposits (Figs. 1d and17b). A series of relatively closely spaced, arcuate crest lines identified on the western side of the glen are thought to represent the crests of recessional moraines, possibly representing minor (?seasonal) readvances during the overall southward retreat of the Loch Killin glacier. The relatively thick sequence of glacial deposits laid down earlier with the narrow part of the valley may have formed an effective barrier enabling the formation of a proglacial lake (Fig. 17b) as the ice-margin retreated into the overdeepening now occupied by Loch Killin. This lake may have been fed by meltwater streams emanating from ice retreating onto the higher ground to the east of the glen, and would have expanded as the ice continued to retreat southwards (Fig. 17c). However, the maximum size of this lake is uncertain due to the absence of any preserved palaeo-shorelines. Eventually it is likely that the glacigenic sediments forming the dam to this lake were breached enabling the lake to drain northwards via the valley now occupied by the River Fechlin (Fig. 17c). This interpretation, therefore, agrees with the model of deglaciation proposed by Merritt *et al*. (2013).

Implications for using micromorphology to establish the depositional setting of glacigenic diamictons

A number of the previously published studies have attempted to use this technique to discriminate between diamictons deposited in different sedimentary environments by systematically recording the type and frequency of microstructures (e.g. Carr 2001, 2004; Lee, 2001; Carr *et al*., 2001; Menzies *et al*. 2006; Menzies and Whiteman 2009; Kilfeather *et al*., 2010; Linch *et al*., 2012). The resultant summary tables have been used to compare the range of microfabrics and structures present within diamictons laid down in radically different sedimentary environments. In particular, this approach has been applied offshore in an attempt to discriminate between diamictons formed in glacimarine environments (Carr 2001; Carr *et al*., 2001; Kilfeather *et al*., 2010). In these studies the context to the thin sections taken from cores may only be provided by the lithological log of the borehole, with the broader context being provided by either subsurface profiles (seismic data) and/or multibeam survey data of the seabed. One significant drawback of the application of micromorphology to establish the depositional setting of glacigenic sediments is the fact that the identification of the various microstructures (see van der Meer, 1987, 1993; Menzies, 1998, 2000; Menzies *et al*., 2006) can be rather subjective and dependent upon the experience of the person carrying out the analysis (see Leighton *et al*., 2012). Furthermore, sediment composition can have a profound effect on the range of microstructures present; for example plasmic fabrics will only develop where clay minerals are present within the matrix. Consequently, this can lead to the miss identification and/or characterisation of the depositional setting of the diamicton.

Importantly the results of the present and previously published studies clearly indicate that the range of microstructures present within mass flow diamictons (Lachniet *et al*., 2001; Phillips, 2006; Reinardy and Lukas, 2009) are comparable to those found within subglacially deformed tills (see Phillips *et al*., 2011, 2013; 2018a and b; Vaughan-Hirsch *et al*., 2013; Neudorf *et al*., 2015; Brumme, 2015; Gehrmann *et al*., 2017; Narloch *et al*., 2020). These structures include clast microfabrics, pressure shadows, folds, laminations, shears, faults and water-escape structures, as well as 'turbate' structures. Lachniet *et al*. (2001), in particular, emphasised the fact that while deformation microstructures in subglacial sediments can be described in tectonic terms, some of the same structures occur in mass flow deposits (unaffected by over-riding ice) were they are primary in origin and result from sedimentary processes. This has important implications for anyone trying to use micromorphology, on its own, to establish the depositional setting of glacigenic diamictons. So although micromorphology is providing valuable insights into the processes occurring during the deposition/formation of both modern and ancient glacigenic sedimentary sequences, this approach should not be used in isolation, but as part of a multidisciplinary approach, involving sedimentological, geomorphological and structural field techniques.

Conclusions

Macroscale sedimentological and structural field observations combined with micromorphological and micro-structural analysis of a sequence of Late Devensian (Weichselian) sands, gravels and diamictons exposed within a recessional moraine near Loch Killin (near Fort Augustus, NE Scotland) have provided valuable insights into the ice-marginal processes which led to the construction of this landform. Microstructures present within the stratified diamictons mantling the glacitectonised core of the moraine provide evidence of clast microfabric development in response to ductile shearing during the emplacement of these ice-marginal mass flows. Deformation was preferentially partitioned into the matrix of the diamicton, with shearing occurring throughout the entire mass flow as it flowed towards the WNW. This microscale evidence suggests that these deposits represent Type 4 wet sediment (water-rich) flows (Lachniet *et al*., 1999). The moraine is cut by a number of steeply inclined sediment-filled hydrofractures. These laminated infills are interpreted as having accommodated several phases of fluid flow, with a palaeoflow direction towards the WNW. Construction of this moraine has been divided into three stages: **Stage 1** equates to a readvance of the glacier from the ESE/SE with glacitectonism (folding and thrusting) of a pre-existing sequence of diamictons and glacifluvial outwash resulting from WNW/NW-directed ice-push; **Stage 2** is characterised by the deposition of a sequence of the ice-marginal glacifluvial and mass flows deposits during a period of still-stand, accompanied by melting and down wasting of the snout which lay immediately to the

ESE/SE; and **Stage 3** leading to the development of a network of sediment-filled hydrofractures which allowed overpressurised meltwater to escape from beneath the ice, probably during the initial stages of retreat. This complex sequence of events leading to the construction of the recessional moraine are thought to have occurred during the early stages of the deglaciation of the study area and the southward retreat of the “Loch Killin glacier”.

Acknowledgements

Jonathan Lee and Andrew Finlayson are thanked for their constructive comments on an earlier version of this paper. John Fletcher at the BGS thin section laboratory is acknowledged for his expertise in making the thin sections of the unlithified sediments examined during this study. This paper is published with permission of the Director of the British Geological Survey.

References

Baroni, C., Fasano, F., 2006. Micromorphological evidence of warm-based glacier deposition from the Ricker Hills Tillite (Victoria Land, Antarctica). Quaternary Science Reviews. 25, 976-992.

Benn, D.I., Evans, D.J.A. 2010. Glaciers and Glaciation. Arnold, London 802 pp.

Benediktsson, Í.Ö., Möller, P., Ingólfsson, Ó., van der Meer, J.J.M., Kjær, K.H., Krüger, J., 2008. Instantaneous end moraine and sediment wedge formation during the 1890 glacier surge of Brúarjökull, Iceland. Quaternary Science Reviews 27, 209-234. DOI: https://doi.org/10.1016/j.quascirev.2007.10.007.

Boulton, G.S., 2006. Glaciers and their coupling with hydraulic and sedimentary processes. In Knight, P. G. (ed.) Glacier Science and Environmental Change, 3–22. Blackwell, Oxford.

Boulton, G.S., Eyles, N. 1979. Sedimentation by valley glaciers: a model and genetic classification. In Schlüchter, C. (ed.) Moraines and varves. Balkema, Rotterdam, 11-23.

Boston, C.M., 2012. A glacial geomorphological map of the Monadhliath Mountains, Central Scottish Highlands. Journal of Maps, 8(4), 437-444.

Boston, C.M., Lukas, S. 2013. Evidence for ice advance during ice sheet deglaciation and ice-dammed lake formation within Glen Killin. In: Boston, C.M., Lukas, S., Merritt, J.W. (eds.) The Quaternary of the Monadhliath Mountains and the Great Glen. London, UK, Quaternary Research Association, 93-111.

Boston, C.M., Lukas, S., Carr, S.J., 2015. A Younger Dryas plateau ice field in the Monadhliath, Scotland, and implications for regional palaeoclimate. Quaternary Science Reviews, 108, 139-162.

Bradwell, T., Stoker, M.S., Golledge, N.R., Wilson, C.K., Merritt, J.W., Long, D., Everest, J.D., Hestvik, O.B., Stevenson, A.G., Hubbard, A.L., Finlayson A.G., Mathers, H.E. 2008. The northern sector of the last British Ice Sheet: Maximum extent and demise. Earth Science Reviews 88, 207-226.

Bradwell, T., Sigurdsson, O., Everest, J. 2013. Recent, very rapid retreat of a temperate glacier in SE Iceland. Boreas, 42, 959–973.

Brumme, J., 2015. Three-dimensional microfabric analyses of Pleistocene tills from the cliff section Dwasieden on Rügen (Baltic Sea coast): micromorphological evidence for subglacial polyphase deformation (PhD thesis). Ernst-Moritz-Arndt-Universitstäat, Greifswald, 210 pp.

Carr, S.J., 2001. Micromorphological criteria for distinguishing subglacial and glacimarine sediments: evidence from a contemporary tidewater glacier, Spitsbergen. Quaternary International. 86, 71-79.

Carr, S.J., 2004. Micro-scale features and structures. In: D.J.A. Evans, D.I. Benn (eds.) A practical guide to the study of glacial sediments. Arnold, London, pp. 115-144.

Carr, S.J., Haflidason, H., Sejrup, H.P., 2000. Micromorphological evidence supporting late Weichselian glaciation of the northern North Sea. Boreas. 29, 315-328.

Carr, S.J., Holmes, R., van der Meer, J.J.M., Rose, J., 2006. The last glacial maximum in the North Sea basin: Micromorphological evidence of extensive glaciation. Journal of Quaternary Science. 21, 131-153.

Charlesworth, J.K. 1956. The Late-glacial history of the Highlands and islands of Scotland. Transactions of the Royal Society of Edinburgh, 62, 769-933.

Denis, M., Guiraud, M., Konaté, M., Buoncristiani, J.-F. 2010. Subglacial deformation and water-pressure cycles as a key for understanding ice stream dynamics: evidence from the Late Ordovician succession of the Djado Basin (Niger). International Journal of Earth Science (Geol Rundsch). 99, 1399-1425.

Evans, D.J.A. and Twigg, D.R. 2002. The active temperate glacial landsystem: a model based on Breiðamerkurjökull and Fjallsjökull, Iceland. Quaternary Science Reviews, 21, 2143–2177.

Evans, D.J.A., Benn, D.I. 2004. A practical guide to the study of glacial sediments. Arnold, London.

Evans, D.J.A., 2018. Till: A Glacial Process Sedimentology. John Wiley and Sons Ltd, UK.

Feng, Y., Jones, J.F., Gray, K.E. 2015. Pump-in and Flow –back Tests for determination of Fracture Parameters and In-situ Stresses. AADE American association of Drilling Engineers. AADE-15-NTCE-35, 1-11.

Gehrmann, A., Hüneke, H., Meschede, M., Phillips, E. 2017. 3D microstructural architecture of deformed glacigenic sediments associated with large-scale glacitectonism, Jasmund Peninsula (NE Rügen), Germany. Journal of Quaternary Science 32, 213-230. DOI: 10.1002/jqs.2843.

Hart, J.K., 2007. An investigation of subglacial shear zone processes from Weybourne, Norfolk, UK. Quaternary Science Reviews. 26, 2354-2374.

Hewitt, K. 1967. Ice-front deposition and the seasonal effect: a Himalayan example. Transactions of the Institute of British Geographers 42, 93-106.

Hiemstra, J.F., Rijsdijk, K.F., Evans, D.J.A., van der Meer, J.J.M., 2005. Integrated micro- and macro-scale analyses of Last Glacial maximum Irish Sea diamicts from Abermaw and Treath y Mwnt, Wales, UK. Boreas. 34, 61-74.

Hubbard, B., Sharp, M.J., Willis, I.C., Nielsen, M.K., Smart, C.C. 1995. Borehole water level variations and the structure of the subglacial hydrological system of Haut Glacier d'Arolla, Valais, Switzerland. Journal of Glaciology, 41, 572–583.

Khatwa, A., Tulaczyk, S., 2001. Microstructural interpretations of modern and Pleistocene subglacially deformed sediments: the relative role of parent material and subglacial processes. Journal of Quaternary Science 16, 507-517.

Kilfeather, A.A., Ó Cofaigh, C., Dowdeswell, J.A., Meer, J.J.M. van der, Evans, D.J.A., 2010. Micromorphological characteristics of glacimarine sediments: implications for distinguishing genetic processes of massive diamicts. Geo-Marine Letters. 30, 77-97.

Krüger, J. 19915. Origin, chronology and climatological significance of annual moraine ridges at Mýrdalsjökull, Iceland. The Holocene 5, 420-427.

Lachniet, M.S., Larson, G.J., Strasser, J.C., Lawson, D.E., Evenson, E.B., 1999. Microstructures of glacigenic sediment flow deposits, Matanuska Glacier, Alaska. In Mickleson, D.M., Attig, J.W. (Eds). Glacial Processes Past and Present. Geological Society of America, Special Paper. 337, Boulder, CO.

Lachniet, M.S., Larson, G.J., Lawson, D.E. Evenson, E.B., Alley, R.B., 2001. Microstructures of sediment flow deposits and subglacial sediments: a comparison. Boreas. 30, 254-262.

Larsen, N.K., Piotrowski, J.A., Christiansen, F., 2006. Microstructures and micro-shears as proxy for strain in subglacial diamicts: implications for basal till formation. Geology. 34, 889-892.

Larsen, N.K., Piotrowski, J.A., Menzies, J., 2007. Microstructural evidence of low-strain, time transgressive subglacial deformation. Journal of Quaternary Science. 22, 593-608.

Lawson, D.E. 1982. Mobilization, movement and deposition of active subaerial sediment flows, Matanuska Glacier, Alaska. Journal of Geology 90, 279-300.

Lee, J.R. 2001. Genesis and palaeogeographical significance of the Corton Diamicton (basal member of the North Sea Drift Formation), East Anglia, U.K. Proceedings of the Geologists' Association 112, 29-43.

Linch, L.D., van der Meer, J.J.M., Menzies, J. 2012. Micromorphology of iceberg scour in clays: Glacial Lake Agassiz, Manitoba, Canada. Quaternary Science Reviews 55, 125-144.

Lukas, S. 2005. A test of the englacial thrusting hypothesis of ‘hummocky’ moraine formation – case studies from the north-west Highlands, Scotland. Boreas 34, 287–307.

Lukas, S. 2012. Processes of annual moraine formation at a temperate alpine valley glacier: insights into glacier dynamics and climatic controls. Boreas 41, 463–480.

Menzies, J., 2000. Micromorphological analyses of microfabrics and microstructures indicative of deformation processes in glacial sediments. In: A.J. Maltman, B. Hubbard, M.J. Hambrey (eds.). Deformation of glacial materials. Geological Society of London, Special Publication 176, 245-257.

Menzies, J., Maltman, A.J., 1992. Microstructures in diamictons - evidence of subglacial bed conditions. Geomorphology. 6, 27-40.

Menzies, J., Whiteman, C., 2009. A comparative analyses of microstructures from Late Jurassic diamictic units, near Helmsdale, northeast Scotland and a Pleistocene diamicton from Milton, southern Ontario, Canada – a differential diagnostic method of sediment typing using micromorphology. Netherlands Journal of Geosciences, Geologie en Mijnbouw. 88, 75-94.

Menzies, J., Zaniewski, K., 2003. Microstructures within a modern debris flow deposit derived from Quaternary glacial diamicton – a comparative micromorphological study. Sedimentary Geology. 157, 31-48.

Menzies, J., Zaniewski, K., Dreger, D., 1997. Evidence from microstructures of deformable bed conditions within drumlins, Chimney Bluffs, New York State. Sedimentary Geology. 111, 161-175.

Menzies, J., van der Meer, J.J.M., 1998. Sedimentological and micromorphological examination of a late Devensian multiple diamicton sequence near Moneydie, Perthshire, east-central Scotland. Scottish Journal of Geology. 34, 15-21.

Menzies, J., van der Meer, J.J.M., Rose, J., 2006. Till – a glacial "tectomict", a microscopic examination of a till's internal architecture. Geomorphology 75, 172-200.

Merritt, J.W., Auton, C.A., Firth, C.R., 1995. Ice-proximal glaciomarine sedimentation and sea-level change in the Inverness area, Scotland: a review of the deglaciation of a major ice stream of the British Late Devensian ice sheet. Quaternary Science Reviews, 14(3), 289-329.

Merritt, J.W., Auton, C.AA., Boston, C.M., Everest, J.D., Merritt, J.E. 2013 An overview of the main Late Devensian glaciation of the Central Grampian Highlands. In: Boston, C.M.; Lukas, S., Merritt, J.W., (eds.). The Quaternary of the Monadhliath Mountains and the Great Glen. London, UK, Quaternary Research Association, 25-40.

Mix, A.C., Bard, E., Schneider, R. 2001. Environmental processes of the Ice Age: land, ocean, glaciers (EPILOG). Quaternary Science Reviews 20, 627-657.

Narloch, W., Piotrowski, J.A., Wysota, W., Larsen, N.K., Menzies, J., 2012. The signature of strain magnitude in tills associated with the Vistula Ice Stream of the Scandinavian Ice Sheet, central Poland. Quaternary Science Reviews 57, 105-120.

Narloch, W., Wysota, W., Piotrowski, J.A., 2013. Sedimentological record of subglacial conditions and ice sheet dynamics of the Vistula Ice Stream (north-central Poland) during the Last Glaciation. Sedimentary Geology 293, 30-44.

Narloch, W., Phillips, E., Piotrowski, J.A., Ćwiek, M. 2020. Patterns of deformation within a subglacial shear zone: Implications for palaeo-ice stream bed evolution. Sedimentary Geology 397,

Neudorf, C.M., Brennand, T.A., Lian, O.B., 2013. Till-forming processes beneath parts of the Cordilleran Ice Sheet, British Columbia, Canada: macroscale and microscale evidence and a new statistical technique for analysing microstructure data. Boreas, 10.1111/bor.12009. ISSN 0300-9483.

Passchier, C.W., Trouw, R.A.J., 1996. Microtectonics. Springer.

Phillips, E.R., 2006. Micromorphology of a debris flow deposit: evidence of basal shearing, hydrofracturing, liquefaction and rotational deformation during emplacement. Quaternary Science Reviews. 25, 720-738.

Phillips, E., Merritt, J.W., Auton, C.A., Golledge, N.R., 2007. Microstructures developed in subglacially and proglacially deformed sediments: faults, folds and fabrics, and the influence of water on the style of deformation. Quaternary Science Reviews 26, 1499-1528.

Phillips, E., Merritt, J., 2008. Evidence for multiphase water-escape during rafting of shelly marine sediments at Clava, Inverness-shire, NE Scotland. Quaternary Science Reviews 27, 988–1011.

Phillips, E., Hughes, L., 2014. Hydrofracturing in response to the development of an overpressurised subglacial meltwater system during drumlin formation: an example from Anglesey, NW Wales. Proceedings of the Geologists' Association 125, 296–311.

Phillips E., Lee, J.R. 2011. Description, measurement and analysis of glacitectonically deformed sequences. In Phillips, E., Lee, J.R., Evans, H.M. (eds.) Glacitectonics: Field Guide. Quaternary Research Association ISBN 0 907 780 830.

Phillips, E.R., van der Meer, J.J.M., Ferguson, A., 2011. A new 'microstructural mapping' methodology for the identification and analysis of microfabrics within glacial sediments. Quaternary Science Reviews 30, 2570-2596.

Phillips, E.R., Lipka, E., van der Meer, J.J.M. 2013a. Micromorphological evidence of liquefaction and sediment deposition during basal sliding of glaciers. Quaternary Science Reviews 81, 114-137.

Phillips, E., Everest, J., Reeves, H., 2013b. Micromorphological evidence for subglacial multiphase sedimentation and deformation during overpressurized fluid flow associated with hydrofracturing. Boreas 42, 395–427.

Phillips, E., Evans, D.J.A., van der Meer, J.J.M., Lee, J.R. 2018b. Microscale evidence of liquefaction and its potential triggers during soft-bed deformation within subglacial traction tills. Quaternary Science Reviews 181, 123-143.

Phillips, E., Spagnolo, M., Alasdair C.J. Pilmer, A.C.J., Rea, B.R., Piotrowski, J.A., Ely, J.C., Carr, S., 2018b. Progressive ductile shearing during till accretion within the deforming bed of a palaeo-ice stream. Quaternary Science Reviews 193, 1-23.

Price, R.J. 1970. Moraines at Fjallsjökull, Iceland. Arctic and Alpine Research, 2, 27–42.

Reinardy, B.T.I., Lukas, S., 2009. The sedimentary signature of ice-contact sedimentation and deformation at macro- and micro-scale: A case study from NW Scotland. Sedimentary Geology. 221, 87-98.

Roberts, D.H., Hart, J.K., 2005. The deforming bed characteristics of a stratified till assemblage in north East Anglia, UK: investigating controls on sediment rheology and strain signatures. Quaternary Science Reviews. 24, 123-140.

Sharp, M. 1984. Annual moraine ridges at Skálafellsjökull, southeast Iceland. Journal of Glaciology, 30, 82–93.

Skolasińska, K., Rachlewicz, G., Szczuciński, W. 2016. Micromorphology of modern tills in southwestern Spitsbergen – insights into depositional and post-depositional processes. Polish Polar Research 37, 435-456.

Spagnolo, M., Phillips, E., Piotrowski, J.A., Rea, B.R., Clark, C.D., Stokes, C.R., Carr, S.J., Ely, J.C., Ribolini, A., Wysota, W., Szuman, I., 2016. Ice stream motion facilitated by a shallow-deforming and accreting bed. Nature Communications DOI: 10.1038/ncomms10723.

Stephenson, D., Gould, D. 1995. British regional geology: the Grampian Highlands (4th edition). Her Majesties Stationery Office London for the British Geological Survey. pp 261.

Stow, D.A.V. 2007. Sedimentary Rocks in the Field: A Colour Guide. Manson Publishing, London, pp 320.

van der Meer, J.J.M., 1987. Micromorphology of glacial sediments as a tool in distinguishing genetic varieties of till. Geological Survey of Finland Special Paper 3, 77-89.

van der Meer, J.J.M., 1997, Particle and aggregate mobility in till: microscopic evidence of subglacial processes. Quaternary Science Reviews. 16, 827-831.

van der Meer, J.J.M., Menzies, J., Rose, J., 2003. Subglacial till, the deformable glacier bed. Quaternary Science Reviews 22, 1659-1685.

van der Meer, J.J.M., Kjær, K.H., Krüger, J., Rabassa, J., Kilfeather, A.A., 2009. Under pressure: clastic dykes in glacial settings. Quaternary Science Reviews 28, 708-720.

van der Wateren, F.M., Kluiving, S.J., Bartek, L.R., 2000. Kinematic indicators of subglacial shearing. In: A.J. Maltman, B. Hubbard, M.J. Hambrey (eds.) Deformation of glacial materials. Geological Society of London, Special Publication. 176, 259-278.

Vaughan-Hirsch, D.P., Phillips, E., Lee, J.R., Hart, J.K., 2013. Micromorphological analysis of poly-phase deformation associated with the transport and emplacement of glaciotectonic rafts at West Runton, north Norfolk, UK. Boreas 42, 376–394.

Figures

Fig. 1. (a) and **(b)** Maps showing the location of the study area; **(c)** Annotated Google Earth® image showing the location of the Loch Killin Study area and principle ice movement directions within the Great Glen and Strathspey; and **(d)** Simplified superficial geology and geomorphology map of the Loch Killin area draped upon the NEXTMap hillshade Digital Elevation Model (DEM).

Fig. 2. Photomontage and interpretation of the sedimentary and structural architecture of the glacigenic sediments exposed on the northern-side of the River Fechlin [NH 524 113].

Fig. 3. (a) Annotated photograph showing the glacitectonic structures present within the ESE-side of the exposed section shown in Fig. 2; and **(b)** Annotated photograph of the stratified sands, gravels and diamictons exposed at the WNW-end of the section shown in Fig 2.

Fig. 4. (a) Photograph showing a steeply dipping sediment filled hydrofracture cutting the deformed, thinly bedded sands and silts exposed towards the ESE-end of the section; **(b)** Lower hemisphere stereographic plot showing the dip and strike of the hydrofracture margins, and palaeo-flow direction recorded by the cross-laminated sands and silts within the sediment fill; **(c)** and **(d)** Photographs showing the laminated nature of the sediments filling the hydrofracture; **(e)** Photograph showing the location of samples N13916, N13917 and N13918 collected to examine the microscale structure and sedimentology of the fill within the hydrofracture; and **(f)** Photograph showing the location of samples N13919, N13920 and N13821 through the sequence of stratified sands, gravels and diamictons exposed at the WNW-end of the section.

Fig. 5. Annotated high-resolution scan and detailed interpretation of a large format thin section taken from sample N13916 (see text for details). See Fig. 4e for details of the location of this sample.

Fig. 6. Annotated high-resolution scan and detailed interpretation of a large format thin section taken from sample N13917 (see text for details). See Fig. 4e for details of the location of this sample.

Fig. 7. Annotated high-resolution scan and detailed interpretation of a large format thin section taken from sample N13918 (see text for details). See Fig. 4e for details of the location of this sample.

Fig. 8. Detailed graphic logs of the laminated sediments infilling the hydrofracture present within samples N13916, N13917 and N13918.

Fig. 9. (a) to **(c)** Annotated photomicrographs showing the details of the laminated sediment-fill to the hydrofracture: **(a)** Clay-rich sequence developed adjacent to the margin of the hydrofracture, cut by a later sand-filled vein (N13917); **(b)** Lenticular lamination within the sediment-fill to the hydrofracture (N13917); and **(c)** Well-developed cross-lamination within the silt and sand laminae (N13917); and **(d)**

Interpretation of the laminated clay, silt and sand shown in (c) highlighting the change in angle of dip of the foresets within each of the sand laminae and the localised soft-sediment deformation (folding) of the cross-lamination.

Fig. 10. Annotated photomicrographs and associated interpretation showing the details of the well-developed cross-lamination within lenticular sand and silt sand laminae (N13918).

Fig. 11. Annotated high-resolution scan and detailed interpretation of a large format thin section taken from sample N13919 (see text for details). See Fig. 4f for details of the location of this sample.

Fig. 12. Annotated high-resolution scan and detailed interpretation of a large format thin section taken from sample N13920 (see text for details). See Fig. 4f for details of the location of this sample.

Fig. 13. Annotated high-resolution scan and detailed interpretation of a large format thin section taken from sample N13921 (see text for details). See Fig. 4f for details of the location of this sample.

Fig. 14. Diagram showing the proposed model for the progressive infilling of the active hydrofracture as a result of the migration of ripples upwards through the open fracture system (see text for details).

Fig. 15. Diagram showing the detailed internal structure of the stratified diamictons and interbedded sands deposited on the down-ice slope of the recessional moraine. The figure shows the partitioning of ductile shearing into the matrix of the diamicton during mass flow with the larger clasts (rock fragments) acting as ridged bodies during this soft-sediment deformation.

Fig. 16. Conceptual model for the evolution of the moraine located at the northern end of Loch Killin: **Stage 1** – records the readvance of the glacier leading to ice-marginal glacitectonism of a pre-existing sequence of sands, gravels and diamictons; **Stage 2** – a period of still-stand and the deposition of a sequence of outwash sands and gravels and ice-marginal mass flows on the down-ice side of the moraine; and **Stage 3** – hydrofracturing and release of overpressurised meltwater from beneath the ice possibly accompanying initial retreat of the glacier (see text for details).

Fig. 17. Cartoon showing the deglaciation of the Loch Killin area with the possible extent of the “Loch Killin glacier”, glacigenic sediments and proglacial lake draped upon the NEXTMap hillshade Digital Elevation Model (DEM).

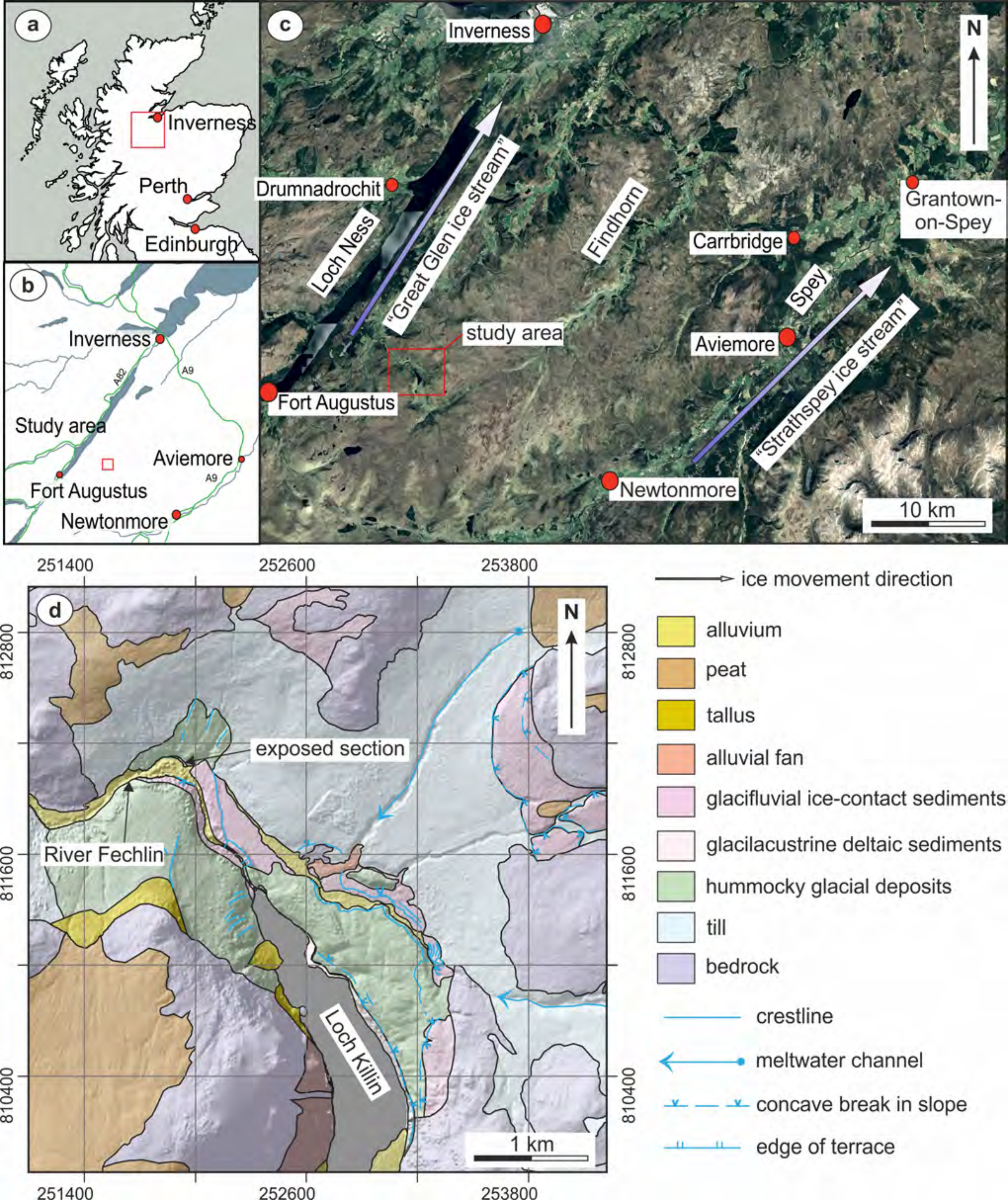

a
Inverness
Perth
Edinburgh
b
Inverness
A82
A9
Study area
Aviemore
A9
Fort Augustus
Newtonmore
c
Inverness
N
Drumnadrochit
Loch Ness
"Great Glen ice stream"
Findhorn
Grantown-on-Spey
Carrbridge
Spey
study area
Aviemore
Fort Augustus
"Strathspey ice stream"
Newtonmore
10 km
d
251400
252600
253800
812800
811600
810400
N
exposed section
River Fechlin
Loch Killin
1 km
ice movement direction
alluvium
peat
tallus
alluvial fan
glacifluvial ice-contact sediments
glacilacustrine deltaic sediments
hummocky glacial deposits
till
bedrock
crestline
meltwater channel
concave break in slope
edge of terrace

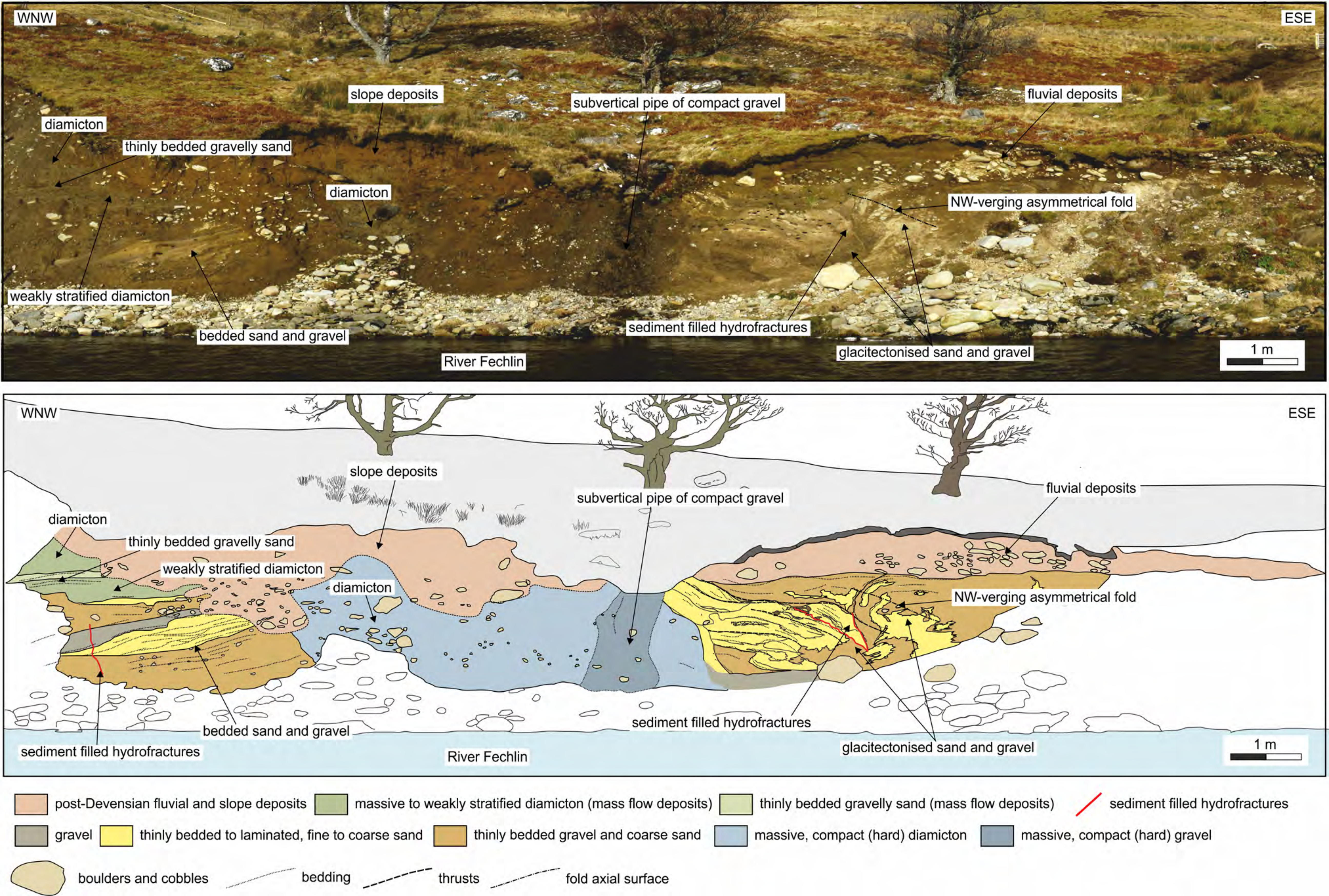
WNW
ESE
slope deposits
subvertical pipe of compact gravel
fluvial deposits
diamicton
thinly bedded gravelly sand
diamicton
NW-verging asymmetrical fold
weakly stratified diamicton
bedded sand and gravel
sediment filled hydrofractures
glacitectonised sand and gravel
River Fechlin
1 m
WNW
ESE
slope deposits
subvertical pipe of compact gravel
fluvial deposits
diamicton
thinly bedded gravelly sand
weakly stratified diamicton
diamicton
NW-verging asymmetrical fold
bedded sand and gravel
sediment filled hydrofractures
sediment filled hydrofractures
glacitectonised sand and gravel
River Fechlin
1 m
post-Devensian fluvial and slope deposits
massive to weakly stratified diamicton (mass flow deposits)
thinly bedded gravelly sand (mass flow deposits)
sediment filled hydrofractures
gravel
thinly bedded to laminated, fine to coarse sand
thinly bedded gravel and coarse sand
massive, compact (hard) diamicton
massive, compact (hard) gravel
boulders and cobbles
bedding
thrusts
fold axial surface

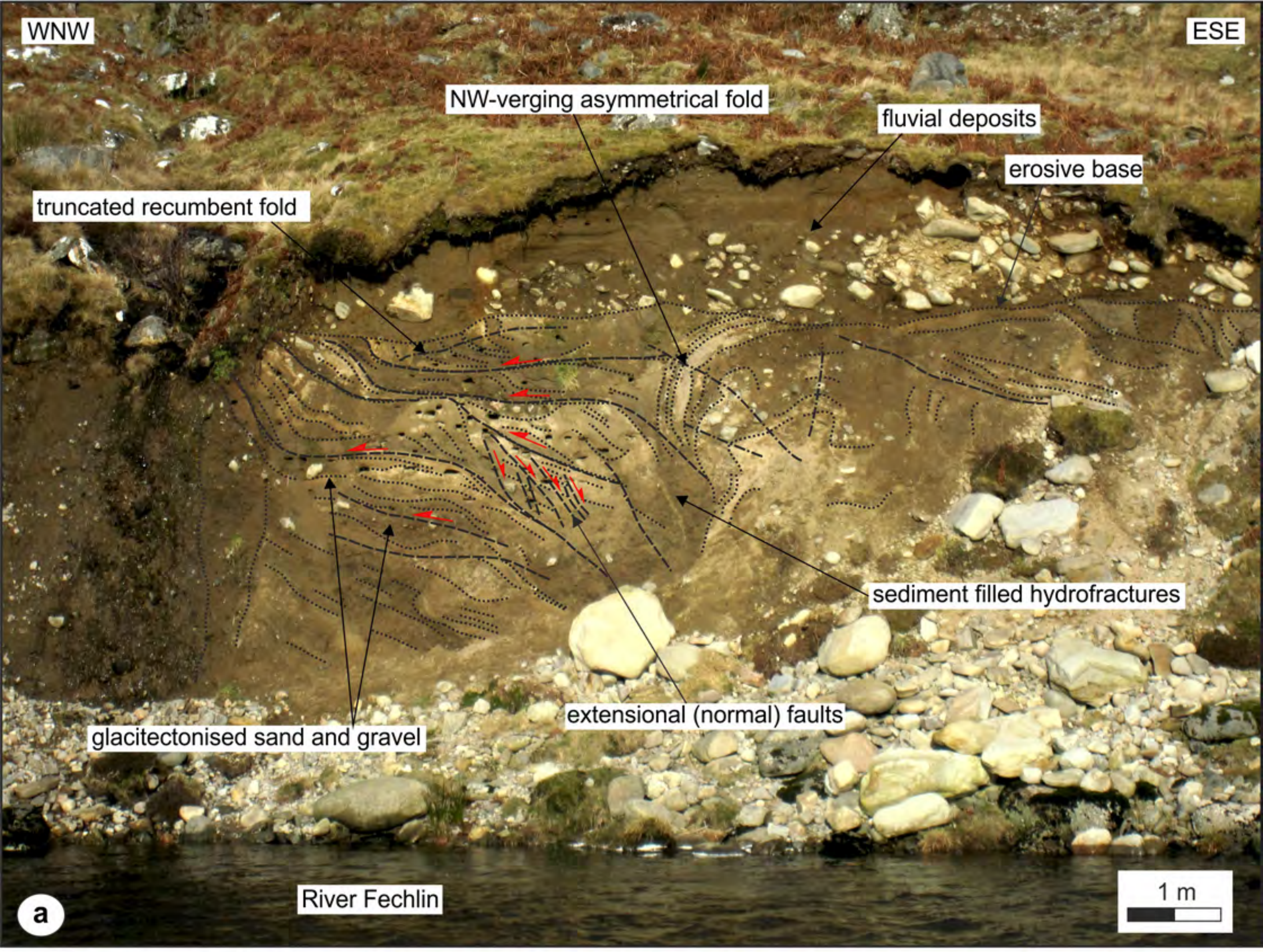
WNW
ESE
NW-verging asymmetrical fold
fluvial deposits
erosive base
truncated recumbent fold
sediment filled hydrofractures
extensional (normal) faults
glacitectonised sand and gravel
River Fechlin
1 m
a

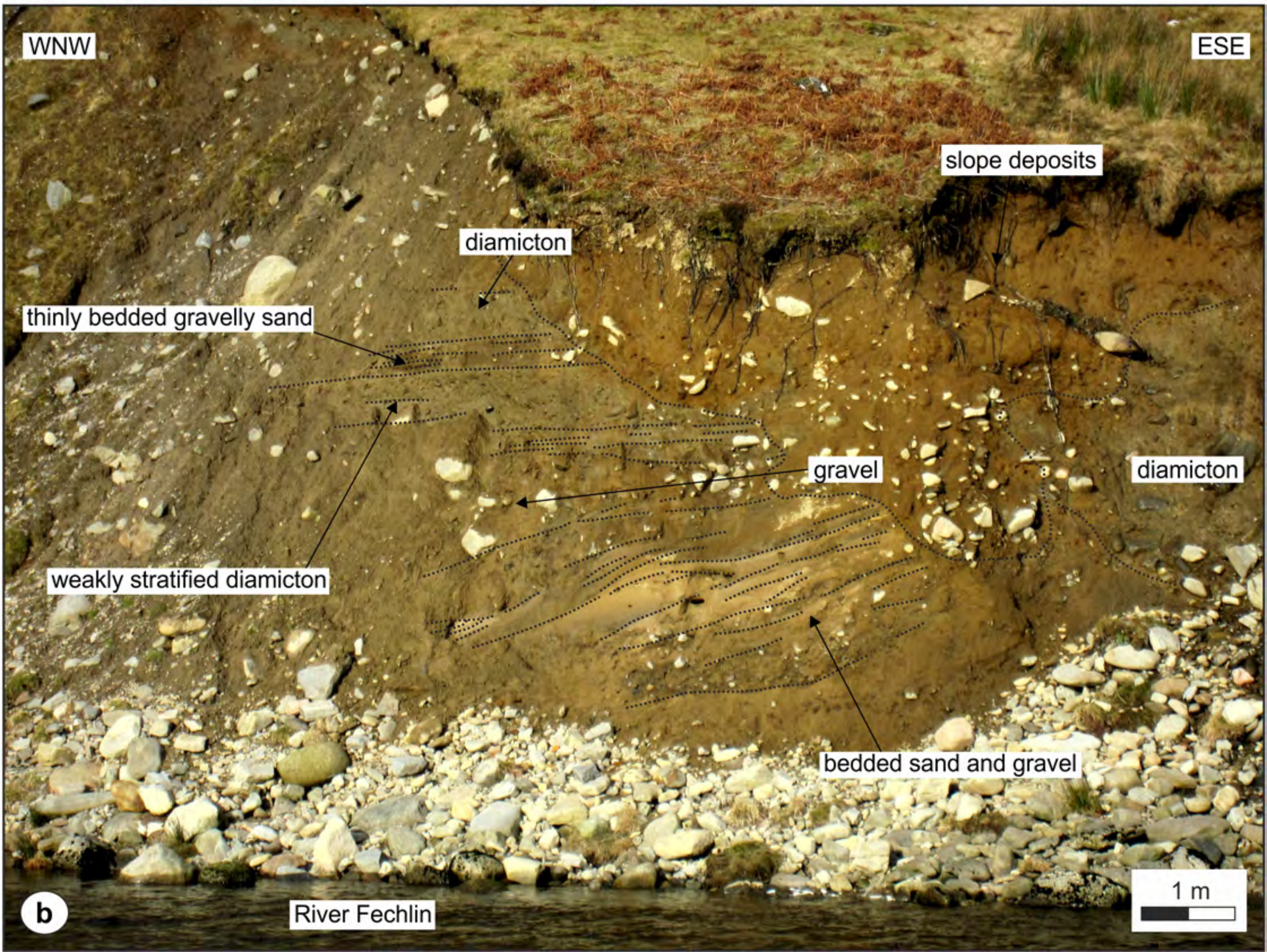
WNW
ESE
slope deposits
diamicton
thinly bedded gravelly sand
gravel
diamicton
weakly stratified diamicton
bedded sand and gravel
River Fechlin
1 m
b

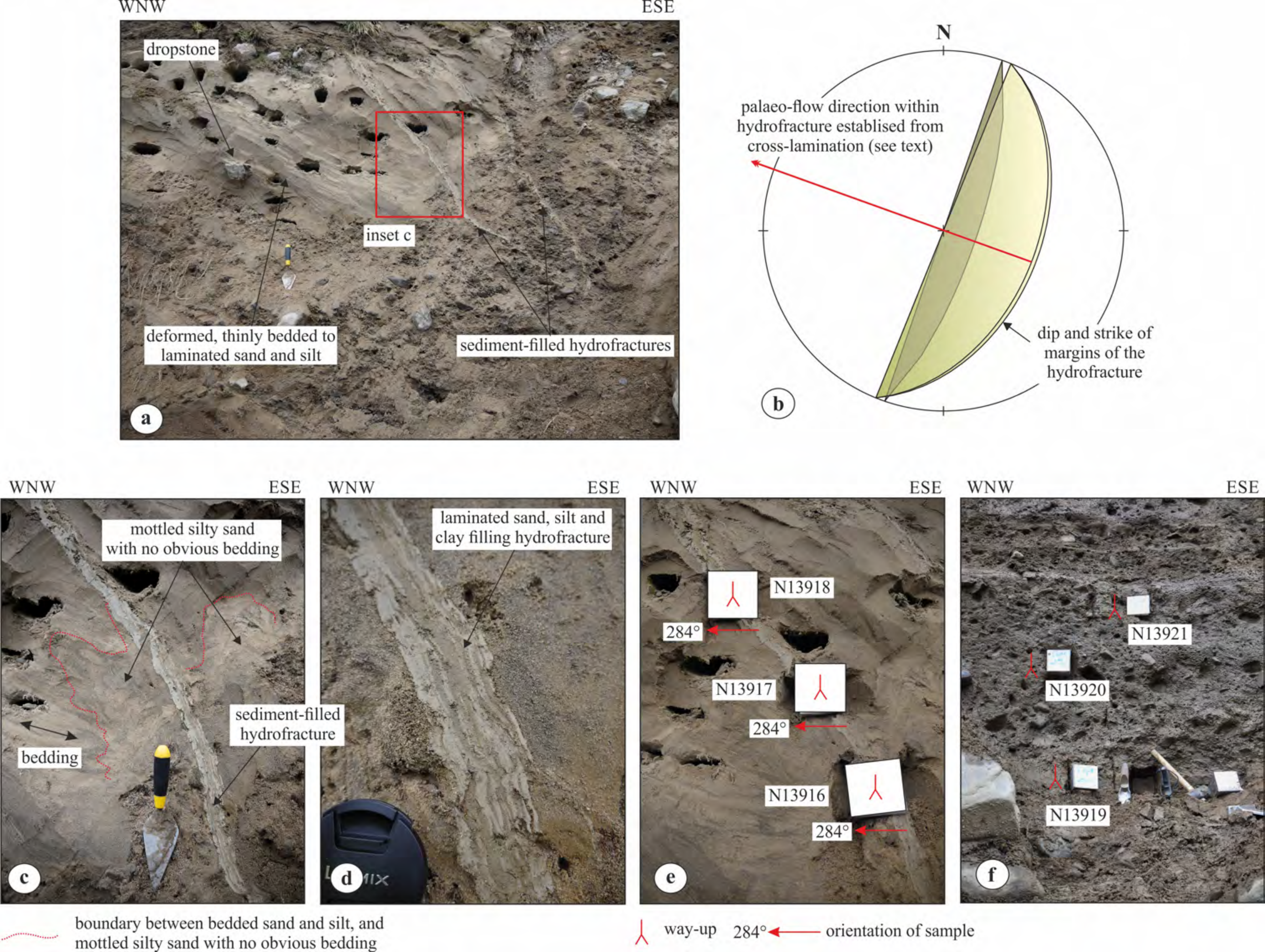
WNW
ESE
dropstone
inset c
deformed, thinly bedded to laminated sand and silt
sediment-filled hydrofractures
a
N
palaeo-flow direction within hydrofracture establised from cross-lamination (see text)
dip and strike of margins of the hydrofracture
b
WNW
ESE
mottled silty sand with no obvious bedding
bedding
sediment-filled hydrofracture
c
WNW
ESE
laminated sand, silt and clay filling hydrofracture
d
WNW
ESE
N13918
284°
N13917
284°
N13916
284°
e
WNW
ESE
N13921
N13920
N13919
f
boundary between bedded sand and silt, and mottled silty sand with no obvious bedding
way-up
284°
orientation of sample

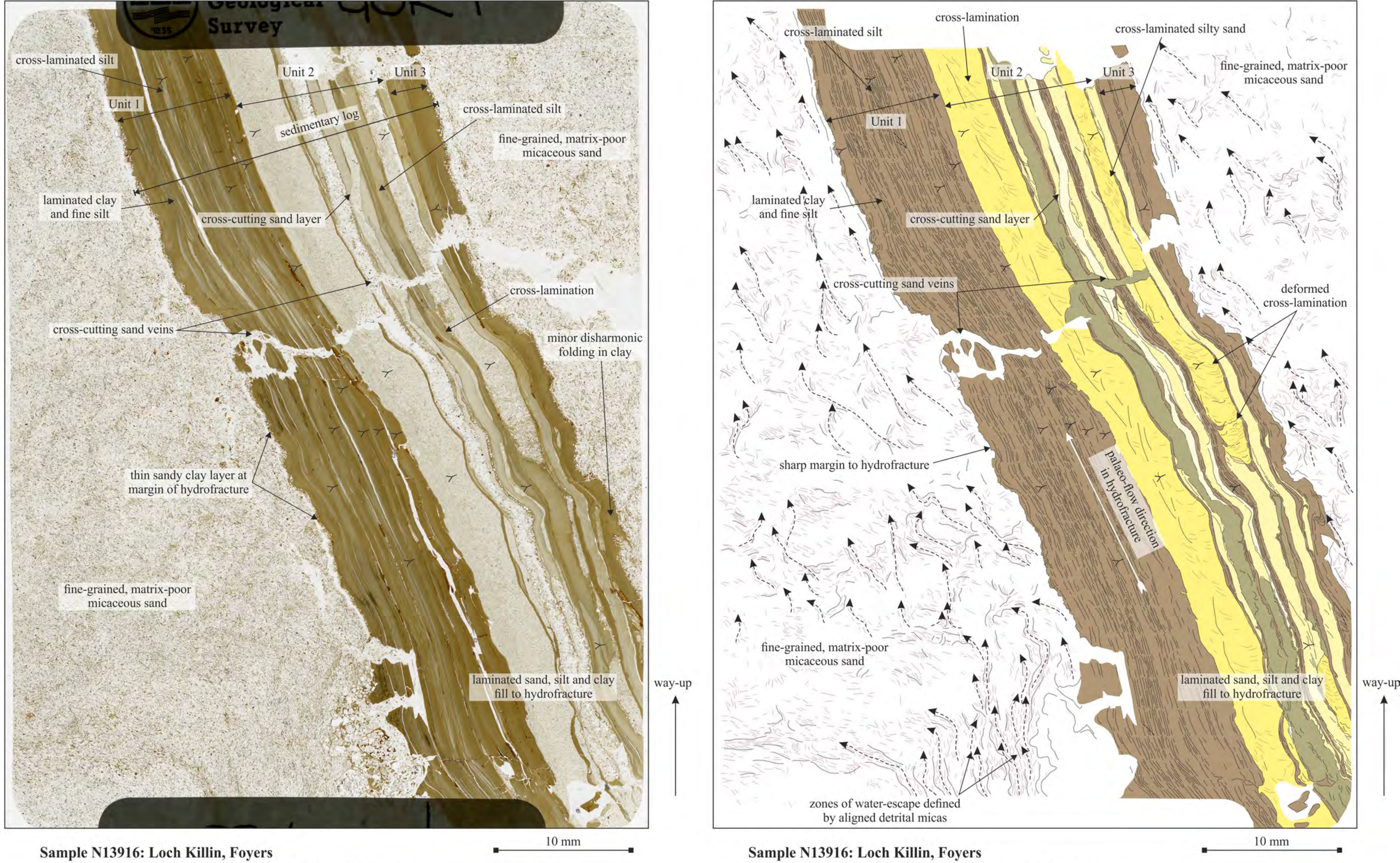

Sample N13916: Loch Killin, Foyers orientation 284 degrees

Sample N13916: Loch Killin, Foyers orientation 284 degrees

way-up indicated by graded bedding and cross lamination; bedding; minor fault; fluid pathway/water-escape defined by alined detrital micas; foliation defined by alined detrital micas

laminated clay and very fine silt/silty clay; medium- to coarse-grained, matrix-poor sand; coarse-silt to fine-sand; coarse-silt to fine-sand

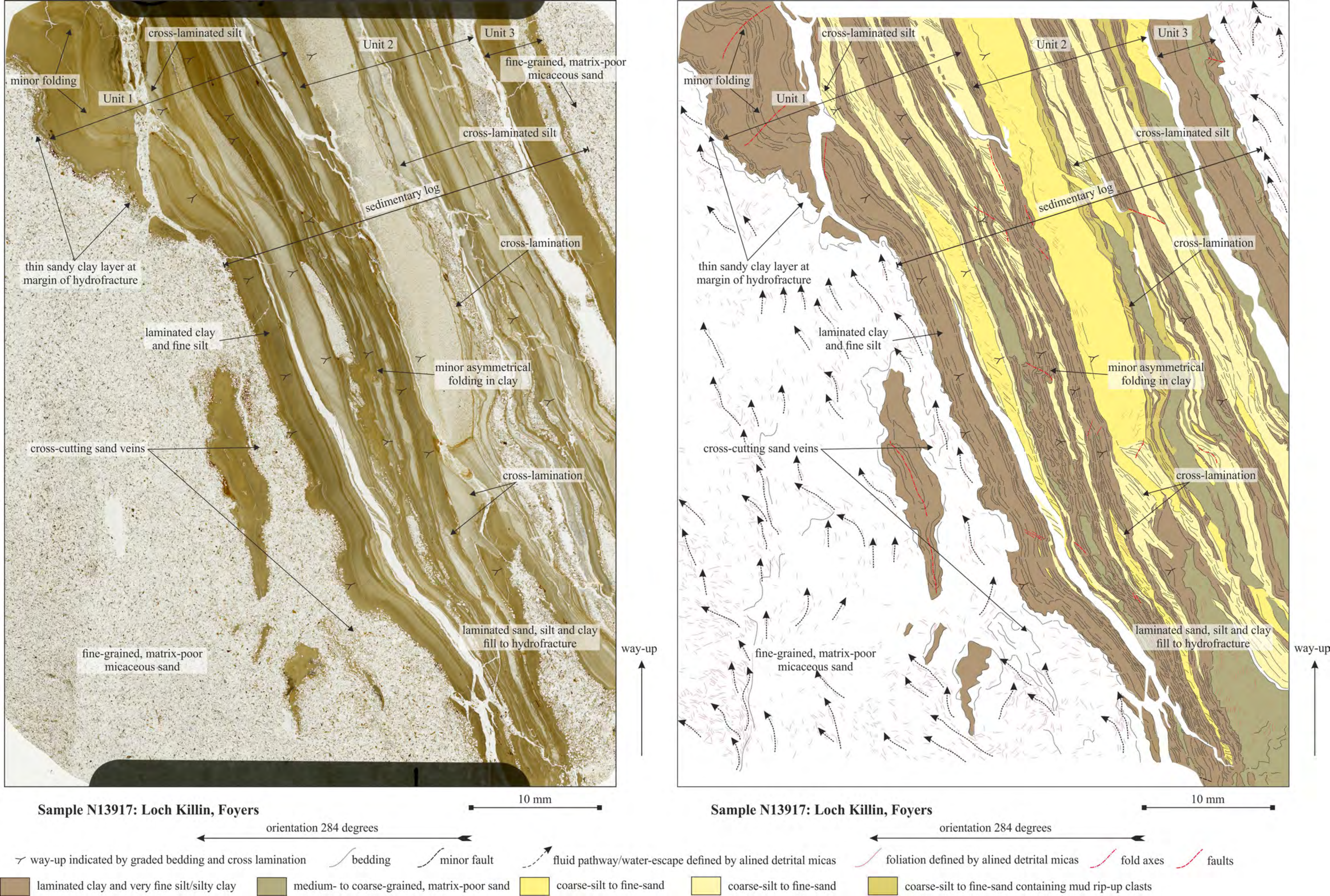
minor folding
cross-laminated silt
Unit 1
Unit 2
Unit 3
fine-grained, matrix-poor micaceous sand
cross-laminated silt
sedimentary log
thin sandy clay layer at margin of hydrofracture
cross-lamination
laminated clay and fine silt
minor asymmetrical folding in clay
cross-cutting sand veins
cross-lamination
laminated sand, silt and clay fill to hydrofracture
fine-grained, matrix-poor micaceous sand
way-up
10 mm
Sample N13917: Loch Killin, Foyers
orientation 284 degrees
way-up indicated by graded bedding and cross lamination
bedding
minor fault
fluid pathway/water-escape defined by alined detrital micas
foliation defined by alined detrital micas
fold axes
faults
laminated clay and very fine silt/silty clay
medium- to coarse-grained, matrix-poor sand
coarse-silt to fine-sand
coarse-silt to fine-sand
coarse-silt to fine-sand containing mud rip-up clasts

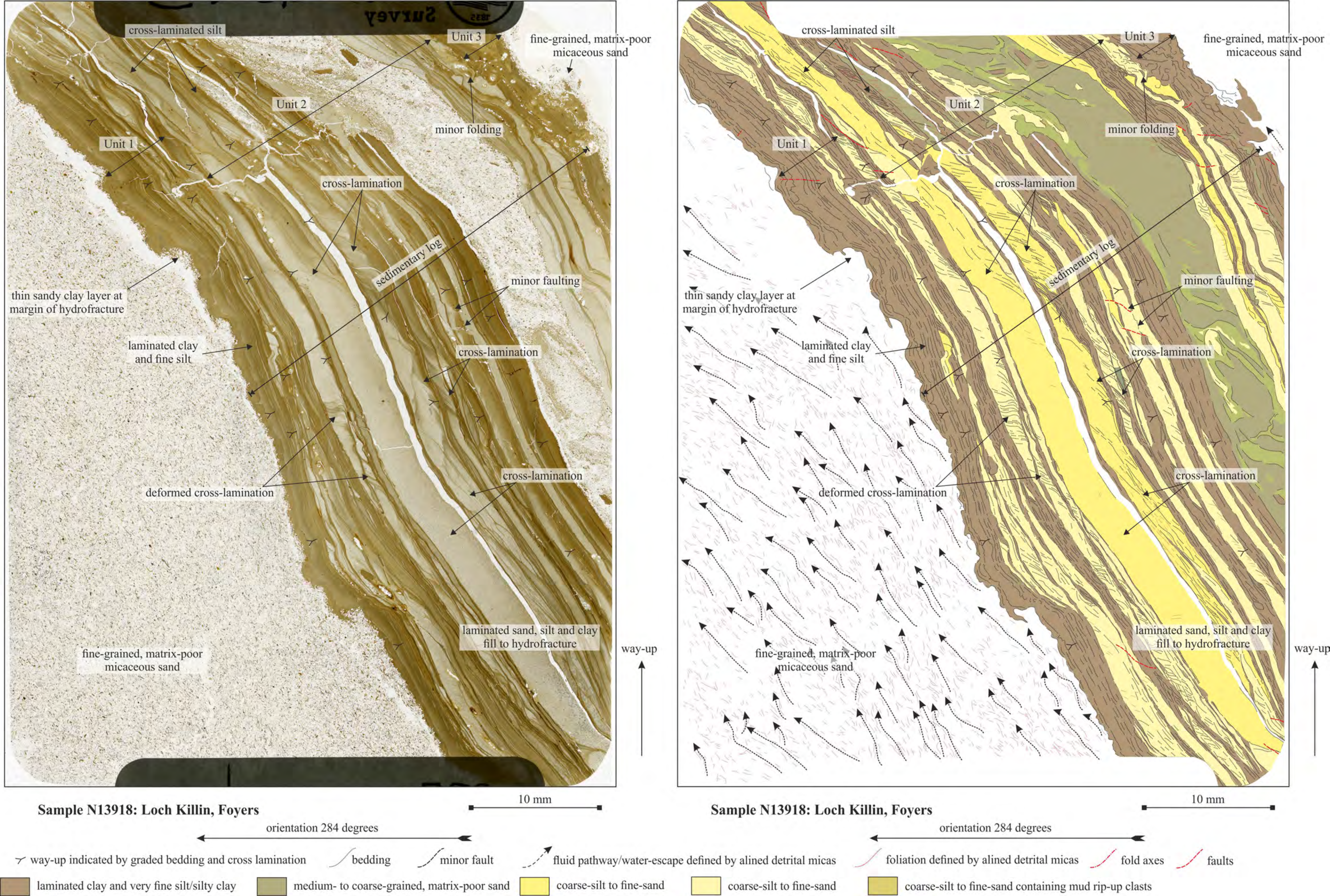
cross-laminated silt
Unit 3
fine-grained, matrix-poor micaceous sand
Unit 2
minor folding
Unit 1
cross-lamination
sedimentary log
thin sandy clay layer at margin of hydrofracture
minor faulting
laminated clay and fine silt
cross-lamination
deformed cross-lamination
cross-lamination
laminated sand, silt and clay fill to hydrofracture
fine-grained, matrix-poor micaceous sand
way-up
10 mm
Sample N13918: Loch Killin, Foyers
orientation 284 degrees
way-up indicated by graded bedding and cross lamination
bedding
minor fault
fluid pathway/water-escape defined by alined detrital micas
foliation defined by alined detrital micas
fold axes
faults
laminated clay and very fine silt/silty clay
medium- to coarse-grained, matrix-poor sand
coarse-silt to fine-sand
coarse-silt to fine-sand
coarse-silt to fine-sand containing mud rip-up clasts

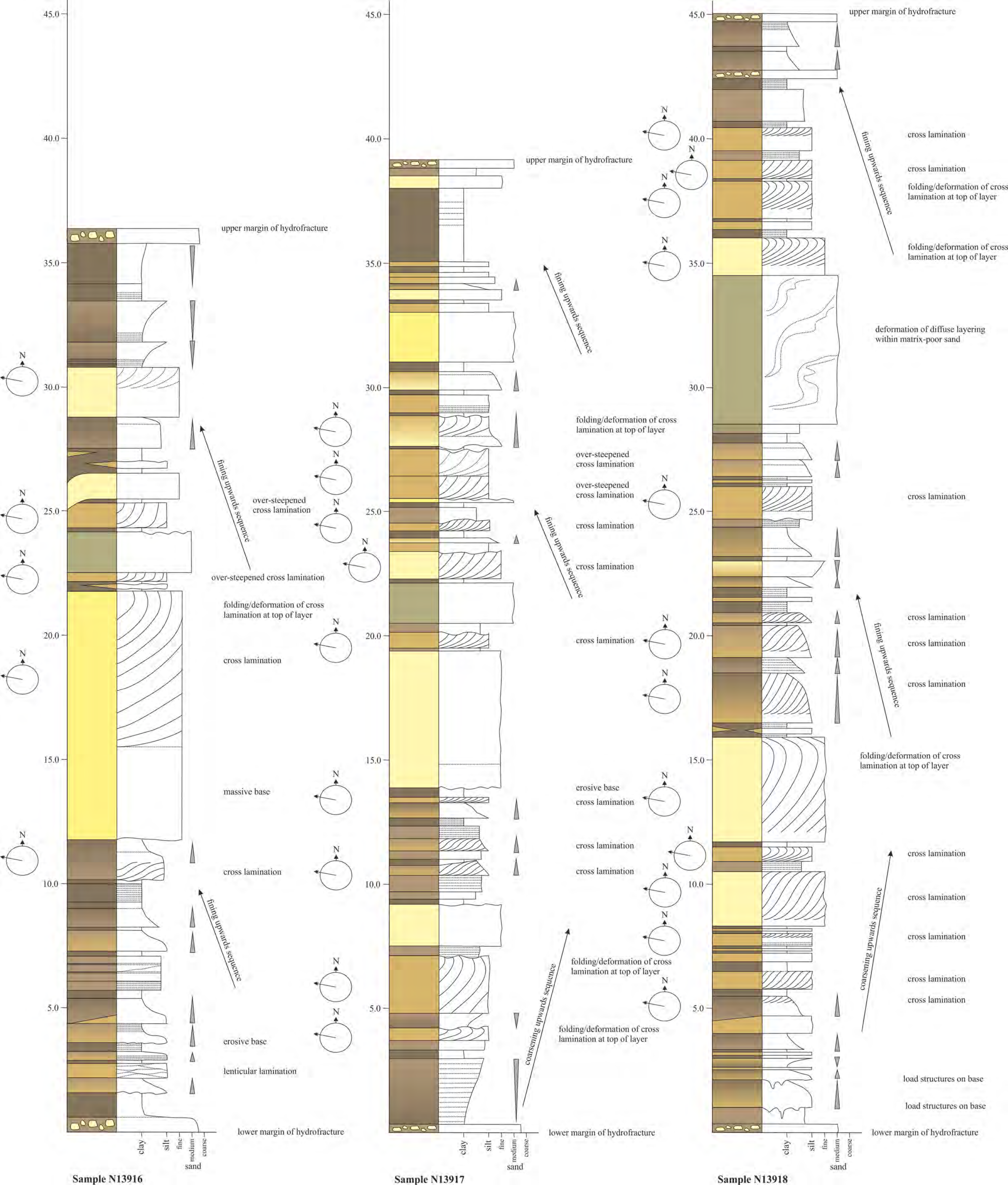

45.0
40.0
35.0
30.0
25.0
20.0
15.0
10.0
5.0
N
upper margin of hydrofracture
fining upwards sequence
over-steepened cross lamination
over-steepened cross lamination
folding/deformation of cross lamination at top of layer
cross lamination
massive base
cross lamination
fining upwards sequence
erosive base
lenticular lamination
lower margin of hydrofracture
clay
silt
fine
medium
coarse
sand
Sample N13916
upper margin of hydrofracture
fining upwards sequence
folding/deformation of cross lamination at top of layer
over-steepened cross lamination
over-steepened cross lamination
cross lamination
cross lamination
fining upwards sequence
cross lamination
erosive base
cross lamination
cross lamination
cross lamination
folding/deformation of cross lamination at top of layer
coarsening upwards sequence
folding/deformation of cross lamination at top of layer
lower margin of hydrofracture
Sample N13917
upper margin of hydrofracture
cross lamination
cross lamination
folding/deformation of cross lamination at top of layer
fining upwards sequence
folding/deformation of cross lamination at top of layer
deformation of diffuse layering within matrix-poor sand
cross lamination
cross lamination
cross lamination
cross lamination
fining upwards sequence
folding/deformation of cross lamination at top of layer
cross lamination
cross lamination
cross lamination
cross lamination
cross lamination
coarsening upwards sequence
load structures on base
load structures on base
lower margin of hydrofracture
Sample N13918

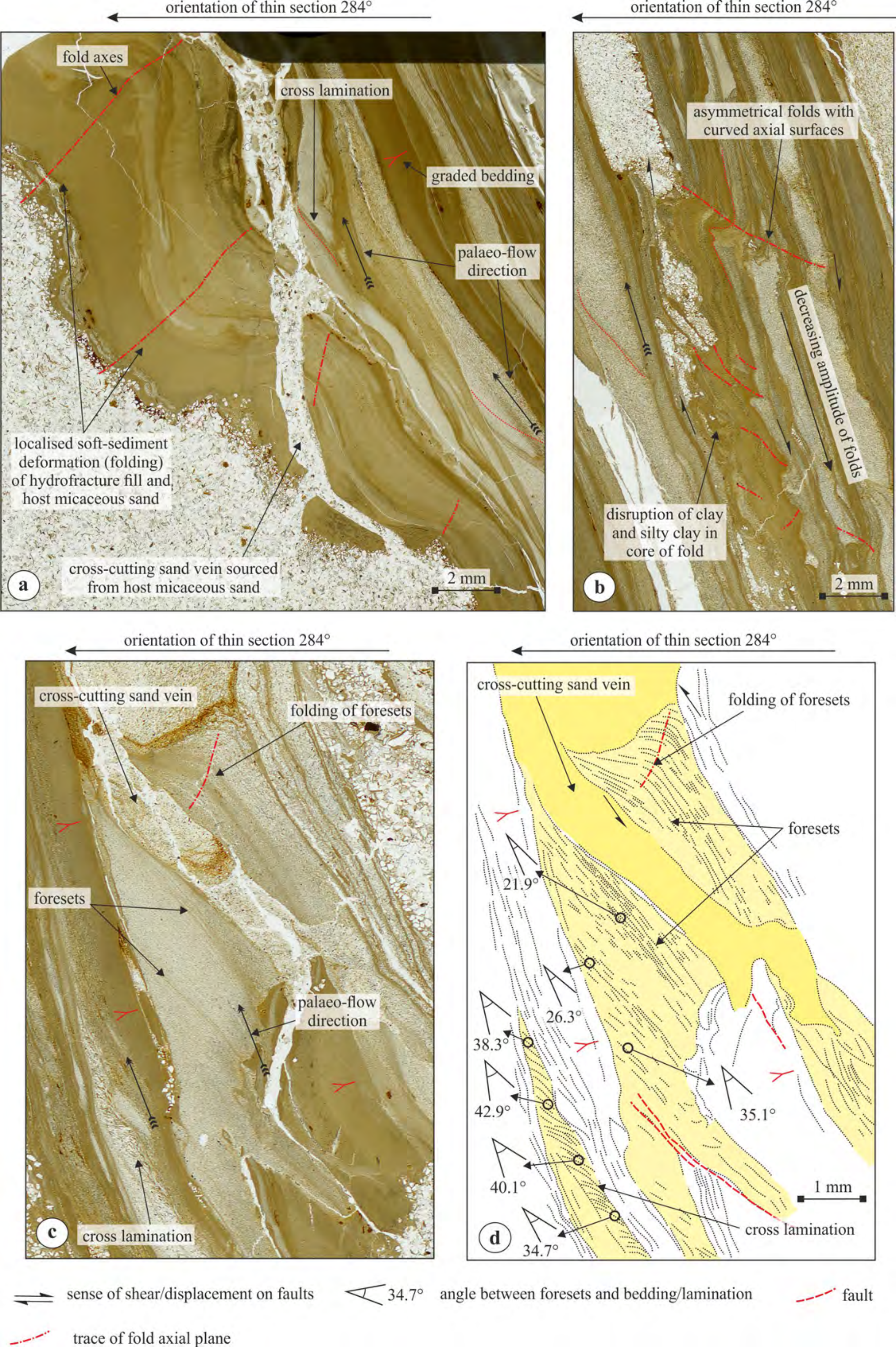

orientation of thin section 284°
fold axes
cross lamination
graded bedding
palaeo-flow direction
localised soft-sediment deformation (folding) of hydrofracture fill and host micaceous sand
cross-cutting sand vein sourced from host micaceous sand
2 mm
a
orientation of thin section 284°
asymmetrical folds with curved axial surfaces
decreasing amplitude of folds
disruption of clay and silty clay in core of fold
2 mm
b
orientation of thin section 284°
cross-cutting sand vein
folding of foresets
foresets
palaeo-flow direction
cross lamination
c
orientation of thin section 284°
cross-cutting sand vein
folding of foresets
foresets
21.9°
26.3°
38.3°
42.9°
40.1°
34.7°
35.1°
1 mm
cross lamination
d
sense of shear/displacement on faults
34.7° angle between foresets and bedding/lamination
fault
trace of fold axial plane

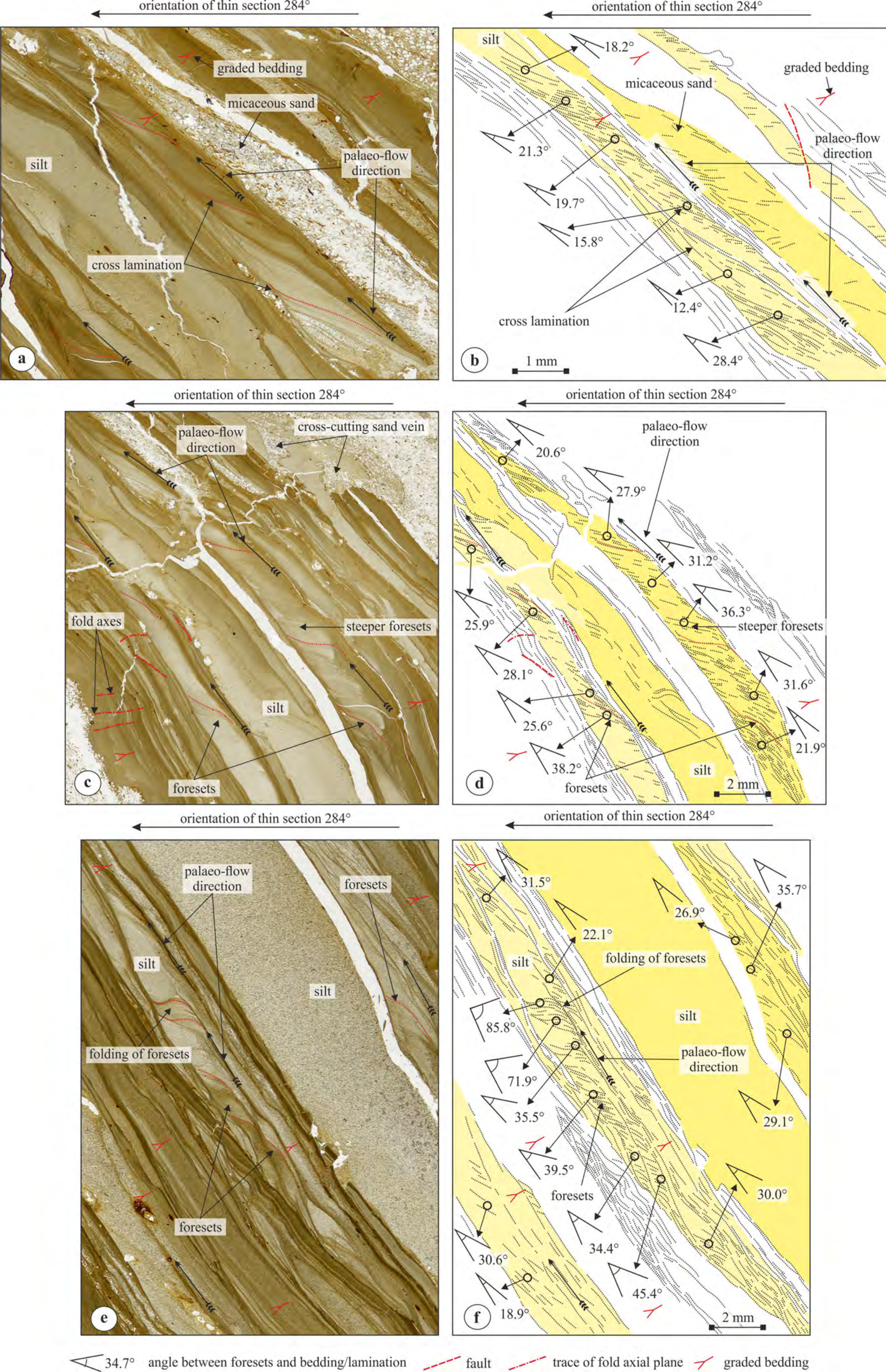
orientation of thin section 284°
graded bedding
micaceous sand
silt
palaeo-flow direction
cross lamination
a
silt
18.2°
21.3°
19.7°
15.8°
12.4°
28.4°
micaceous sand
graded bedding
palaeo-flow direction
cross lamination
b
1 mm
palaeo-flow direction
cross-cutting sand vein
fold axes
steeper foresets
silt
foresets
c
palaeo-flow direction
20.6°
27.9°
31.2°
36.3°
25.9°
28.1°
steeper foresets
31.6°
25.6°
38.2°
21.9°
foresets
silt
d
2 mm
palaeo-flow direction
foresets
silt
folding of foresets
foresets
e
31.5°
22.1°
26.9°
35.7°
silt
folding of foresets
85.8°
71.9°
35.5°
39.5°
palaeo-flow direction
29.1°
foresets
30.0°
34.4°
45.4°
30.6°
18.9°
f
2 mm
34.7° angle between foresets and bedding/lamination
fault
trace of fold axial plane
graded bedding

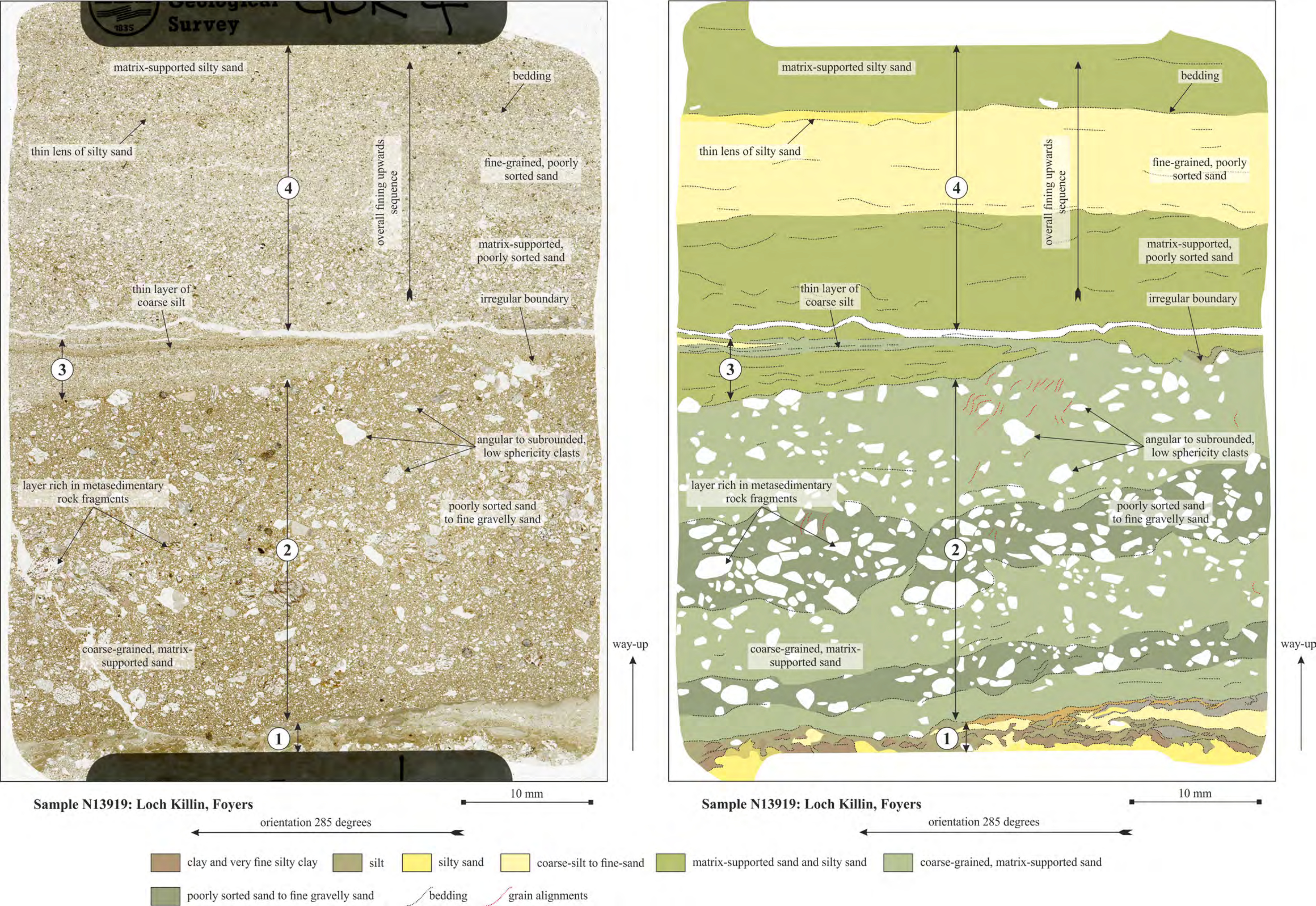

Geological Survey
1835
matrix-supported silty sand
bedding
thin lens of silty sand
fine-grained, poorly sorted sand
overall fining upwards sequence
matrix-supported, poorly sorted sand
thin layer of coarse silt
irregular boundary
angular to subrounded, low sphericity clasts
layer rich in metasedimentary rock fragments
poorly sorted sand to fine gravelly sand
coarse-grained, matrix-supported sand
way-up
1
2
3
4
10 mm
Sample N13919: Loch Killin, Foyers
orientation 285 degrees
clay and very fine silty clay
silt
silty sand
coarse-silt to fine-sand
matrix-supported sand and silty sand
coarse-grained, matrix-supported sand
poorly sorted sand to fine gravelly sand
bedding
grain alignments

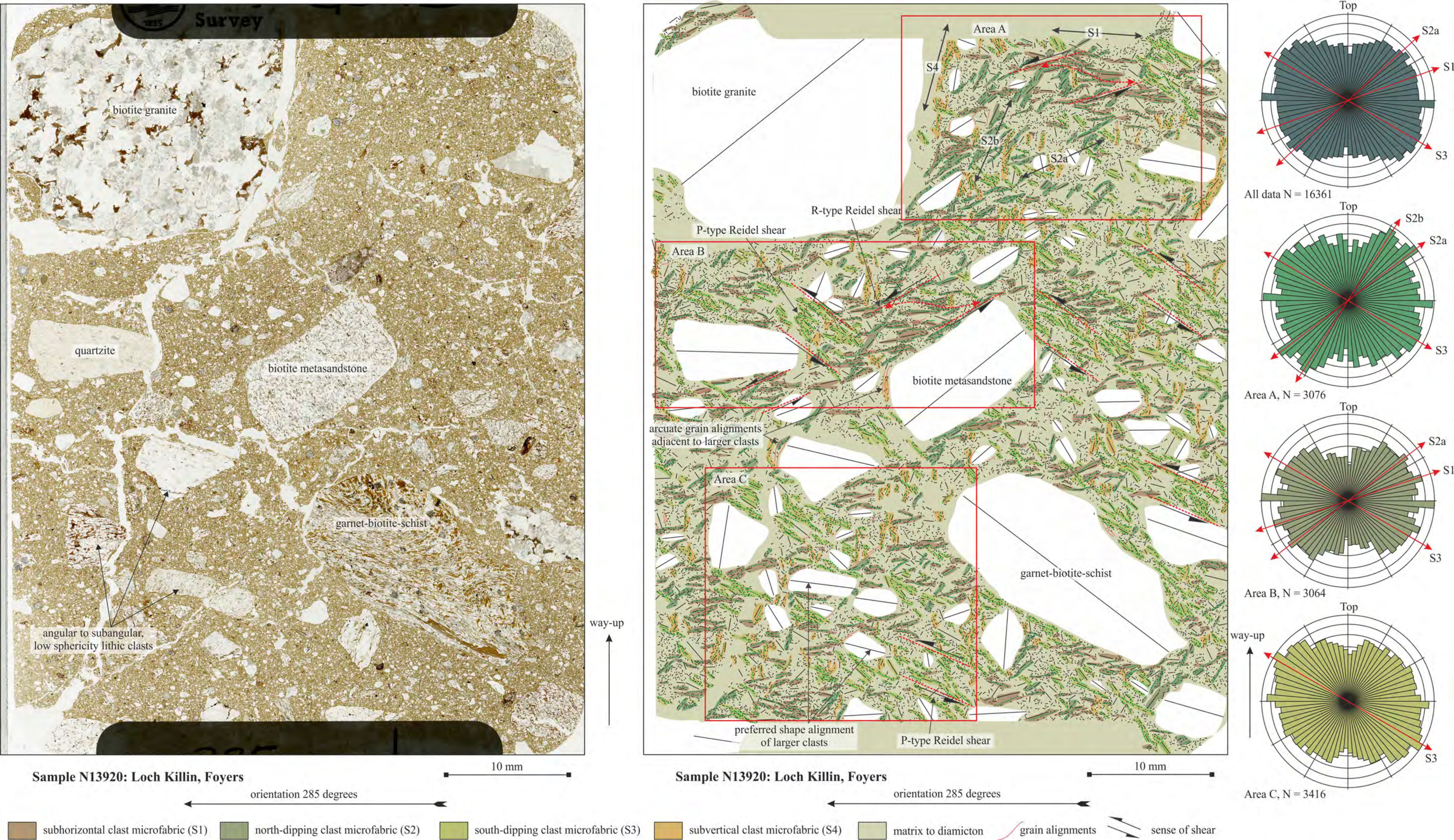
Survey
biotite granite
quartzite
biotite metasandstone
garnet-biotite-schist
angular to subangular,
low sphericity lithic clasts
way-up
Sample N13920: Loch Killin, Foyers
10 mm
orientation 285 degrees
Area A
S1
S4
S2b
S2a
biotite granite
R-type Reidel shear
P-type Reidel shear
Area B
biotite metasandstone
arcuate grain alignments
adjacent to larger clasts
Area C
garnet-biotite-schist
preferred shape alignment
of larger clasts
P-type Reidel shear
Sample N13920: Loch Killin, Foyers
10 mm
orientation 285 degrees
Top
S2a
S1
S3
All data N = 16361
Top
S2b
S2a
S3
Area A, N = 3076
Top
S2a
S1
S3
Area B, N = 3064
way-up
Top
S3
Area C, N = 3416
subhorizontal clast microfabric (S1)
north-dipping clast microfabric (S2)
south-dipping clast microfabric (S3)
subvertical clast microfabric (S4)
matrix to diamicton
grain alignments
sense of shear

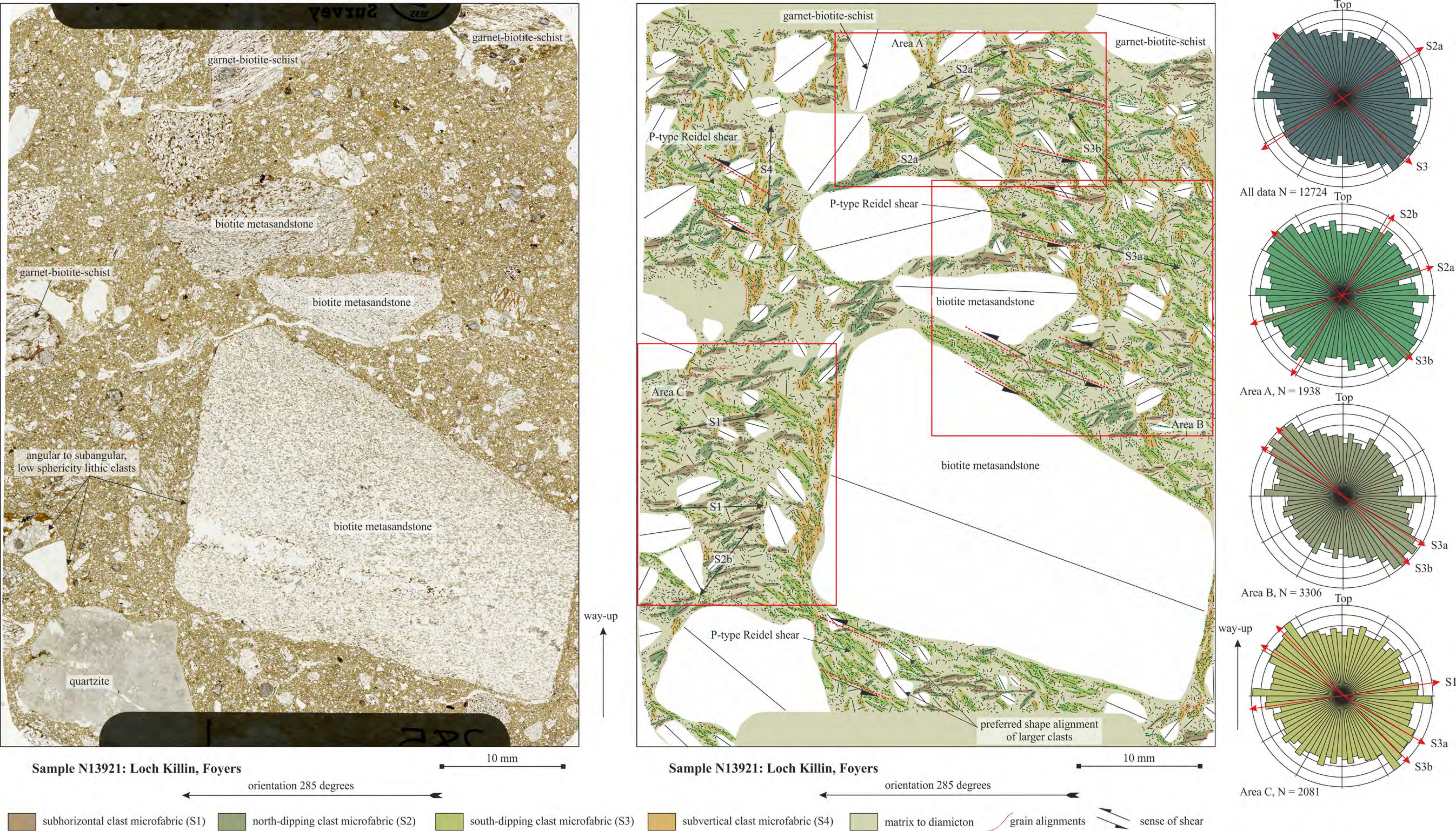
garnet-biotite-schist
garnet-biotite-schist
biotite metasandstone
garnet-biotite-schist
biotite metasandstone
angular to subangular,
low sphericity lithic clasts
biotite metasandstone
quartzite
way-up
10 mm
Sample N13921: Loch Killin, Foyers
orientation 285 degrees
garnet-biotite-schist
Area A
garnet-biotite-schist
S2a
S2a
S3b
P-type Reidel shear
S4
P-type Reidel shear
S3a
biotite metasandstone
Area C
S1
Area B
biotite metasandstone
S1
S2b
P-type Reidel shear
preferred shape alignment
of larger clasts
way-up
10 mm
Sample N13921: Loch Killin, Foyers
orientation 285 degrees
Top
S2a
S3
All data N = 12724
Top
S2b
S2a
S3b
Area A, N = 1938
Top
S3a
S3b
Area B, N = 3306
Top
S1
S3a
S3b
Area C, N = 2081
subhorizontal clast microfabric (S1)
north-dipping clast microfabric (S2)
south-dipping clast microfabric (S3)
subvertical clast microfabric (S4)
matrix to diamicton
grain alignments
sense of shear

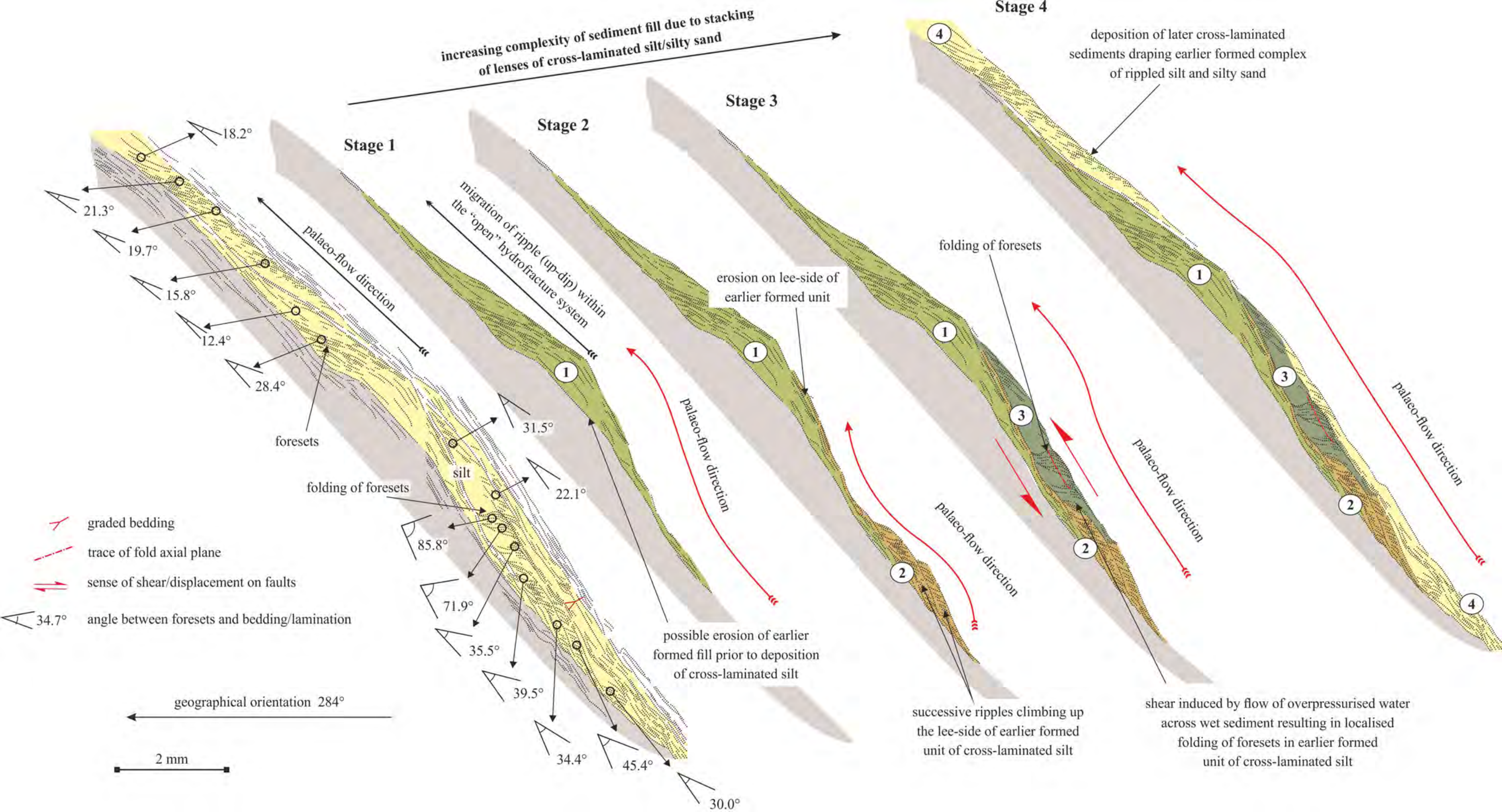

increasing complexity of sediment fill due to stacking of lenses of cross-laminated silt/silty sand
Stage 1
Stage 2
Stage 3
Stage 4
deposition of later cross-laminated sediments draping earlier formed complex of rippled silt and silty sand
18.2°
21.3°
19.7°
15.8°
12.4°
28.4°
31.5°
22.1°
85.8°
71.9°
35.5°
39.5°
34.4°
45.4°
30.0°
palaeo-flow direction
migration of ripple (up-dip) within the "open" hydrofracture system
foresets
silt
folding of foresets
erosion on lee-side of earlier formed unit
folding of foresets
graded bedding
trace of fold axial plane
sense of shear/displacement on faults
34.7° angle between foresets and bedding/lamination
possible erosion of earlier formed fill prior to deposition of cross-laminated silt
successive ripples climbing up the lee-side of earlier formed unit of cross-laminated silt
shear induced by flow of overpressurised water across wet sediment resulting in localised folding of foresets in earlier formed unit of cross-laminated silt
geographical orientation 284°
2 mm

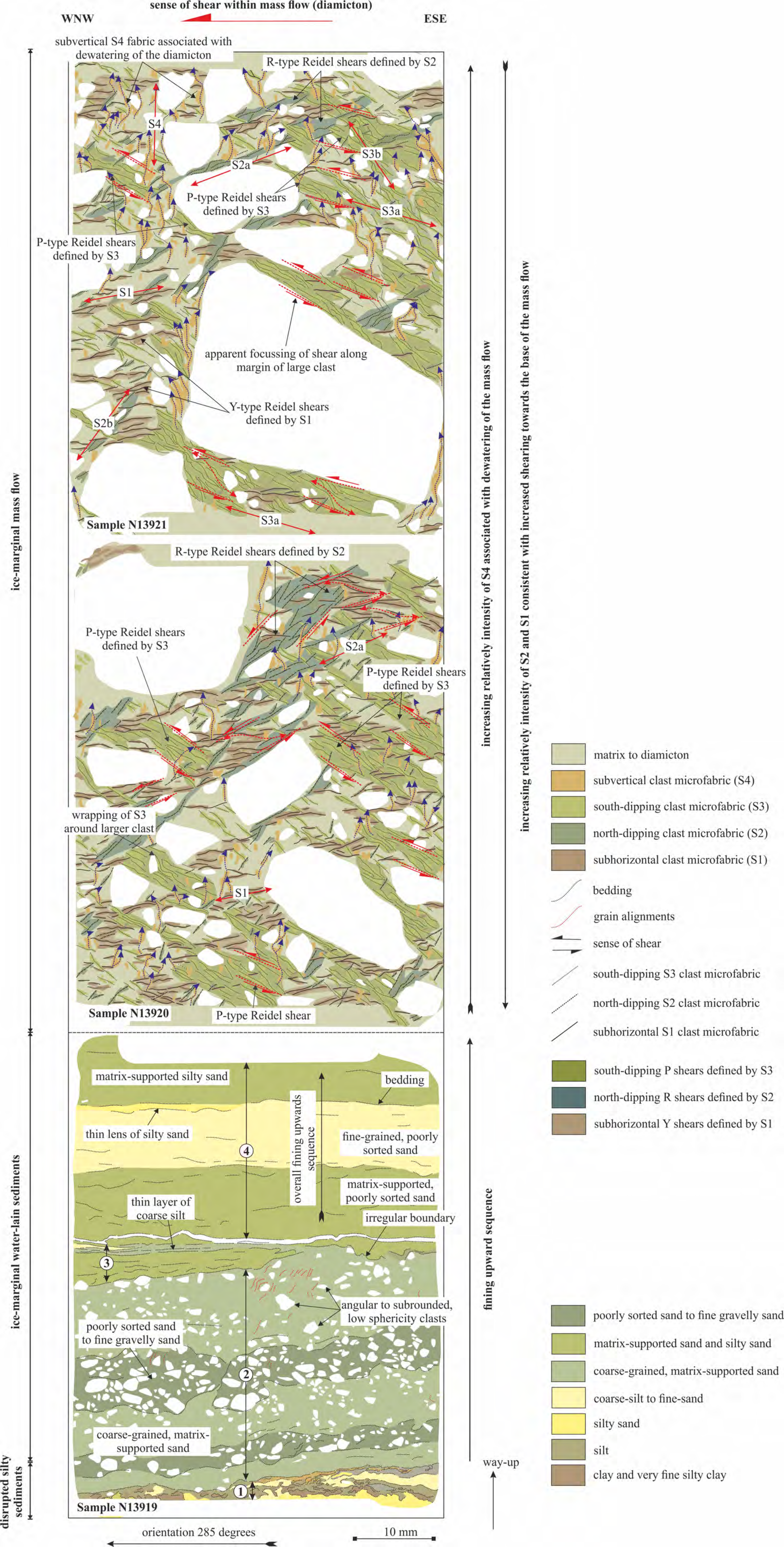

sense of shear within mass flow (diamicton)
WNW
ESE
subvertical S4 fabric associated with dewatering of the diamicton
R-type Reidel shears defined by S2
S4
S3b
S2a
P-type Reidel shears defined by S3
S3a
P-type Reidel shears defined by S3
S1
apparent focussing of shear along margin of large clast
Y-type Reidel shears defined by S1
S2b
Sample N13921
S3a
R-type Reidel shears defined by S2
P-type Reidel shears defined by S3
S2a
P-type Reidel shears defined by S3
wrapping of S3 around larger clast
S1
Sample N13920
P-type Reidel shear
matrix-supported silty sand
bedding
thin lens of silty sand
overall fining upwards sequence
fine-grained, poorly sorted sand
matrix-supported, poorly sorted sand
thin layer of coarse silt
irregular boundary
4
3
angular to subrounded, low sphericity clasts
poorly sorted sand to fine gravelly sand
2
coarse-grained, matrix-supported sand
1
Sample N13919
orientation 285 degrees
10 mm
ice-marginal mass flow
ice-marginal water-lain sediments
disrupted silty sediments
increasing relatively intensity of S4 associated with dewatering of the mass flow
increasing relatively intensity of S2 and S1 consistent with increased shearing towards the base of the mass flow
fining upward sequence
way-up
matrix to diamicton
subvertical clast microfabric (S4)
south-dipping clast microfabric (S3)
north-dipping clast microfabric (S2)
subhorizontal clast microfabric (S1)
bedding
grain alignments
sense of shear
south-dipping S3 clast microfabric
north-dipping S2 clast microfabric
subhorizontal S1 clast microfabric
south-dipping P shears defined by S3
north-dipping R shears defined by S2
subhorizontal Y shears defined by S1
poorly sorted sand to fine gravelly sand
matrix-supported sand and silty sand
coarse-grained, matrix-supported sand
coarse-silt to fine-sand
silty sand
silt
clay and very fine silty clay

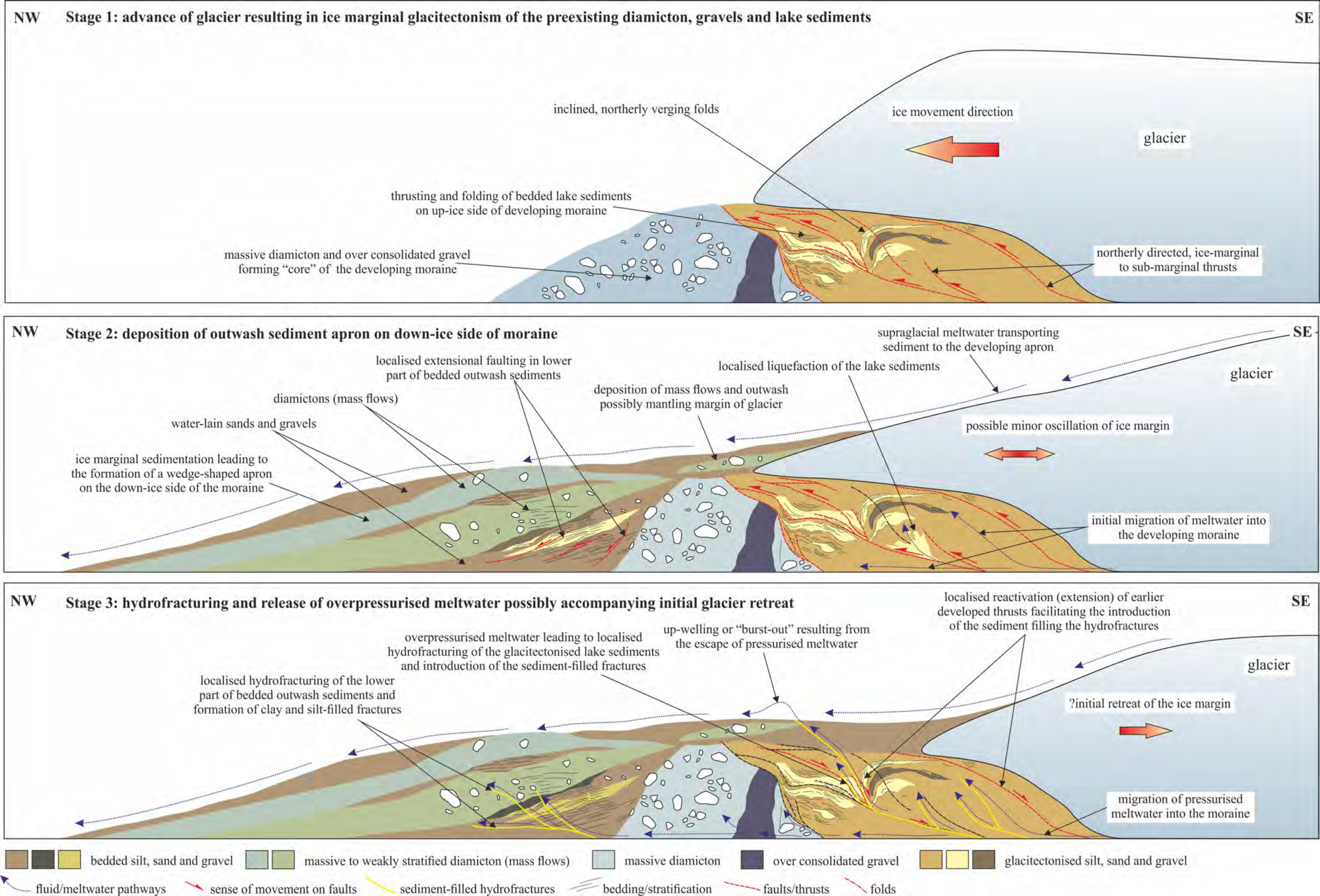

NW
Stage 1: advance of glacier resulting in ice marginal glacitectonism of the preexisting diamicton, gravels and lake sediments
SE
inclined, northerly verging folds
ice movement direction
glacier
thrusting and folding of bedded lake sediments on up-ice side of developing moraine
massive diamicton and over consolidated gravel forming "core" of the developing moraine
northerly directed, ice-marginal to sub-marginal thrusts
NW
Stage 2: deposition of outwash sediment apron on down-ice side of moraine
SE
supraglacial meltwater transporting sediment to the developing apron
localised extensional faulting in lower part of bedded outwash sediments
localised liquefaction of the lake sediments
glacier
diamictons (mass flows)
deposition of mass flows and outwash possibly mantling margin of glacier
water-lain sands and gravels
possible minor oscillation of ice margin
ice marginal sedimentation leading to the formation of a wedge-shaped apron on the down-ice side of the moraine
initial migration of meltwater into the developing moraine
NW
Stage 3: hydrofracturing and release of overpressurised meltwater possibly accompanying initial glacier retreat
SE
localised reactivation (extension) of earlier developed thrusts facilitating the introduction of the sediment filling the hydrofractures
overpressurised meltwater leading to localised hydrofracturing of the glacitectonised lake sediments and introduction of the sediment-filled fractures
up-welling or "burst-out" resulting from the escape of pressurised meltwater
glacier
localised hydrofracturing of the lower part of bedded outwash sediments and formation of clay and silt-filled fractures
?initial retreat of the ice margin
migration of pressurised meltwater into the moraine
bedded silt, sand and gravel
massive to weakly stratified diamicton (mass flows)
massive diamicton
over consolidated gravel
glacitectonised silt, sand and gravel
fluid/meltwater pathways
sense of movement on faults
sediment-filled hydrofractures
bedding/stratification
faults/thrusts
folds

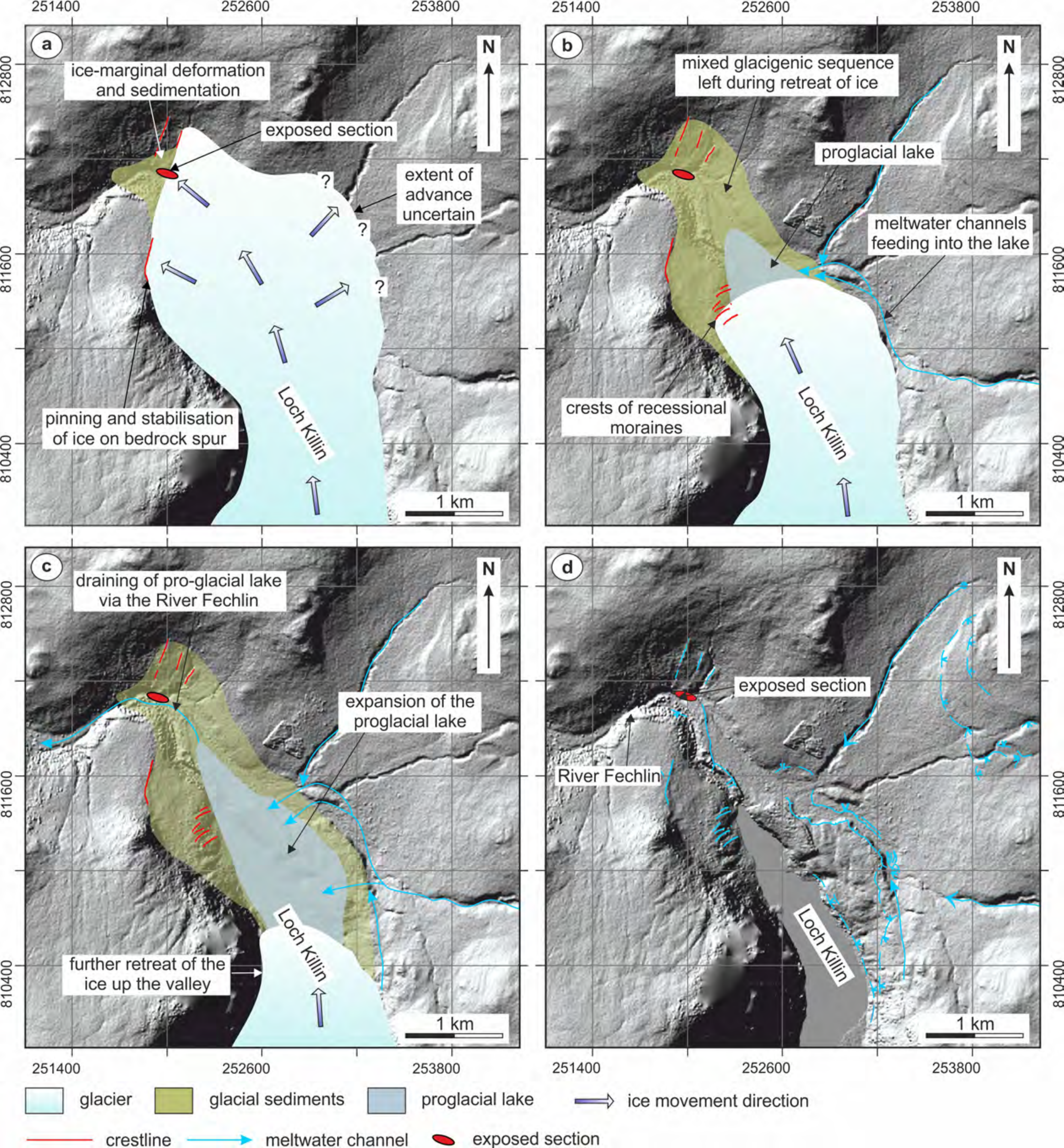

a
b
c
d
N
251400
252600
253800
812800
811600
810400
ice-marginal deformation and sedimentation
exposed section
extent of advance uncertain
?
pinning and stabilisation of ice on bedrock spur
Loch Killin
1 km
mixed glacigenic sequence left during retreat of ice
proglacial lake
meltwater channels feeding into the lake
crests of recessional moraines
draining of pro-glacial lake via the River Fechlin
expansion of the proglacial lake
further retreat of the ice up the valley
River Fechlin
glacier
glacial sediments
proglacial lake
ice movement direction
crestline
meltwater channel
exposed section